J Bone Miner Metab (2006) 24:274–282
DOI 10.1007/s00774-006-0684-1

ORIGINAL ARTICLE

Wataru Ando · Jun Hashimoto · Akihide Nampei
Hideki Tsuboi · Kosuke Tateishi · Takeshi Ono
Norimasa Nakamura · Takahiro Ochi · Hideki Yoshikawa

Imatinib mesylate inhibits osteoclastogenesis and joint destruction in rats with collagen-induced arthritis (CIA)

Received: July 27, 2005 / Accepted: January 6, 2006

Abstract Macrophage colony-stimulating factor (M-CSF) is a key factor for osteoclastogenesis at the bone–pannus interface in patients with rheumatoid arthritis as well as a receptor activator of NF-κB ligand (RANKL). Imatinib mesylate inhibits the phosphorylation of c-*fms*, a receptor for M-CSF. The present study investigates the effect of imatinib mesylate on joint destruction in rats with collagen-induced arthritis (CIA) and on osteoclastogenesis in vitro. Imatinib mesylate (50 or 150 mg/kg), dexamethasone, or vehicle was administered daily to CIA rats for 4 weeks from the onset of arthritis. Hind-paw swelling and body weight were measured weekly. At weeks 2 and 4, the metatarsophalangeal (MTP) joints and the ankle and subtalar joints were radiographically and histologically assessed. The effect of imatinib mesylate on osteoclast formation from rat bone marrow cells with M-CSF and soluble RANKL (sRANKL) in vitro was also examined. Radiographic assessment showed that 150 mg/kg imatinib mesylate suppressed the destruction of the MTP and the ankle and subtalar joints at week 2, and MTP joint destruction at week 4 in CIA rats, although hind-paw swelling was not suppressed. The number of TRAP-positive cells at the bone–pannus interface was significantly reduced in the group administered with 150 mg/kg imatinib mesylate compared with that given vehicle at week 4. Imatinib mesylate dose-dependently inhibited the proliferation of M-CSF-dependent osteoclast precursor cells in vitro as well as osteoclast formation induced by M-CSF and sRANKL. These findings suggest that imatinib mesylate could prevent joint destruction in patients with rheumatoid arthritis.

W. Ando · J. Hashimoto (✉) · A. Nampei · H. Tsuboi · K. Tateishi · T. Ono · N. Nakamura · H. Yoshikawa
Department of Orthopaedics, Osaka University Graduate School of Medicine, 2-2 Yamadaoka, Suita 565-0871, Japan
Tel. +81-6-6879-3552; Fax +81-6-6879-3559
e-mail: junha@ort.med.osaka-u.ac.jp

T. Ochi
National Hospital Organization, Sagamihara National Hospital, Sagamihara, Japan

Key words imatinib mesylate · M-CSF · osteoclast · CIA · rheumatoid arthritis

Introduction

Rheumatoid arthritis (RA) is a chronic and progressive inflammatory disease that is associated with joint destruction. Histopathological characterization of bone erosion in patients with RA and in animal models of inflammatory arthritis such as collagen-induced arthritis (CIA) has provided powerful evidence that bone-resorbing osteoclasts play an important role in the structural joint damage involved in inflammatory arthritis [1].

Imatinib mesylate is a signal transduction inhibitor that specifically targets a set of protein tyrosine kinases, for example, abl, c-*kit*, and platelet-derived growth factor receptor (PDGF-R) [2–4]. Imatinib mesylate is widely administered to treat chronic myeloid leukemia (CML) [2] and c-*kit*-positive gastrointestinal stromal tumors [5]. Miyachi et al. recently reported that imatinib mesylate effectively treats not only CML but also concomitant RA [6]. Eklund and Joensuu also showed that imatinib mesylate might have considerable antirheumatic benefits [7].

A therapeutic dose of imatinib mesylate inhibits the phosphorylation of c-*fms*, a receptor for macrophage colony-stimulating factor (M-CSF) [8] that is an essential factor for osteoclast formation [9–12]. Osteoclast precursors express receptor activator of NF-κB (RANK) and differentiate osteoclasts in the presence of receptor activator of NF-κB ligand (RANKL) and M-CSF [13–15]. RA synovial tissues produce M-CSF, RANKL, and various cytokines that could increase osteoclast formation or activity, including interleukin 1-alpha (IL-1α) and -beta (IL-1β), tumor necrosis factor-alpha (TNF-α), IL-6, IL-11, and IL-17 [16–19]. We recently demonstrated that M-CSF secreted by RA synovial cells might play an important role in the pathogenesis under which osteoclast precursors are maintained [20]. Thus, we postulated that imatinib mesylate has an antibone-resorptive effect in RA. Therefore, this study

investigated the effect of imatinib mesylate on arthritis and joint destruction in rats with CIA and on osteoclastogenesis in the presence of M-CSF and sRANKL in vitro.

Materials and methods

Materials

We purchased the listed reagents from the following suppliers: imatinib mesylate (Gleevec) from Novartis (Basel, Switzerland), bovine type II collagen from Cosmo Bio (Tokyo, Japan), dexamethasone and Freund's incomplete adjuvant from Sigma (St. Louis, MO, USA), recombinant human (rh) M-CSF and rh-sRANKL from PeproTech EC (London, UK), alpha-minimum essential medium (α-MEM) and penicillin/streptomycin from Gibco BRL Life Technologies (Rockville, MD, USA), and fetal bovine serum (FBS) from HyClone (Logan, UT, USA). Lewis rats were purchased from Clea Japan (Tokyo, Japan). All procedures complied with the Osaka University Medical School Guidelines for the Care and Use of Laboratory Animals.

Induction of CIA in rats

We induced CIA using the described modified method [21,22]. In brief, 6-week-old female Lewis rats were intradermally sensitized under anesthesia with 0.5 mg bovine type II collagen in 0.5 ml 0.1 M acetic acid at 4°C and emulsified in 0.5 ml cold Freund's incomplete adjuvant. Seven days later, the rats received an intradermal booster injection of half the volume used for sensitization.

Experimental protocol

We investigated whether imatinib mesylate prevents arthritis and joint destruction in vivo in 34 rats with induced CIA. Immediately after hind-paw swelling was visually obvious in all the rats (at 14 days after initial sensitization), 9 rats per group received 50 or 150 mg/kg imatinib mesylate in 0.05% methylcellulose/phosphate-buffered saline (PBS) daily p.o., and 8 rats per group received either daily dexamethasone (5 mg/kg in 0.05% methylcellulose/PBS; positive control) or vehicle (0.05% methylcellulose/PBS; negative control) p.o. until death. Three rats from each group were killed 2 weeks later and the remainder 4 weeks later.

The rats were weighed and hind-paw swelling was measured weekly using a plethysmometer (model TK-101 CMP; Unicom, Chiba, Japan).

Radiologic and histological analysis

At the end of the experiments (week 2 and 4), the hind paws were visualized by imaging on high-speed radiographic film (Fuji Photo Film, Tokyo, Japan), using the MX-20 Specimen Radiography System (Faxitron X-ray, Wheeling, IL, USA). Radiographic scoring criteria were assessed according to a modified method [23], using the following scale: 0, no bone erosion; 1, light (shape of ankle and subtalar joints, or metatarsal head maintained) bone erosion; 2, severe (disordered ankle and subtalar joints or metatarsal head) bone erosion; and 3, ankle and subtalar joints or metatarsal head missing.

The metatarsophalangeal (MTP) joints were fixed with 4% paraformaldehyde, decalcified with ethylene diamine tetraacetic acid (EDTA), and embedded in paraffin; 4-μm sections were stained with hematoxylin and eosin. To investigate the activity of osteoclastic bone resorption in vivo, sections were visualized using a tartrate-resistant acid phosphate (TRAP) staining kit (Hokudo, Sapporo, Japan). Osteoclasts (TRAP-positive multinucleate cells containing three or more nuclei) located at the site of bone destruction were counted.

Osteoclast differentiation assay

Osteoclast differentiation in vitro proceeded as described [24]. Bone marrow cells isolated from 5-week-old female Lewis rats were seeded at a density of 5×10^6 in 10-cm Petri dishes and incubated in α-MEM containing 10% FBS, 1% penicillin/streptomycin, and 100 ng/ml M-CSF. After a 3-day incubation, nonadherent cells were removed from the cultures by pipetting. Adherent cells (3×10^5) were seeded again in 10-cm culture dishes and incubated in the same medium including 100 ng/ml M-CSF. Cells maintained in M-CSF for an additional 3 days were used as osteoclast precursors and seeded at a density of 1×10^4/well in 48-well plates in the presence of M-CSF (100 ng/ml) and sRANKL (100 ng/ml). Cultures were incubated in quadruplicate with changes of medium on days 2 and 4, and then osteoclast formation was evaluated on day 5. Imatinib mesylate (0.125, 0.25, 0.5, 1, 2, and 4 μM) was added to some cultures during this period, and then the cells were fixed and stained using a TRAP staining kit. Multinucleated TRAP-positive cells with three or more nuclei were counted as mature osteoclasts under a microscope (Eclipse TE 300; Nikon, Tokyo, Japan).

The effect of imatinib mesylate on the calcified matrix resorption activity of osteoclast-like cells was assessed using calcium hydroxyapatite-coated slides (BD BioCoat Osteologic; BD Biosciences, Bedford, MA, USA). Imatinib mesylate (1 μM) was added at day 5 when osteoclasts had already differentiated in the presence of M-CSF and sRANKL. After an additional 5 days of culture with imatinib mesylate, the cells were removed by vigorous washing, and osteological slides were observed by light microscopy (SMZ-U; Nikon) at 1× magnification. The total resorption area on photographs was evaluated using the image analysis software Win ROOF version 3.0 (Mitani, Fukui, Japan).

Proliferation assay of osteoclast precursors

Cell proliferation was evaluated by counting cells and using the Premix WST-1 Cell Proliferation Assay System (Takara

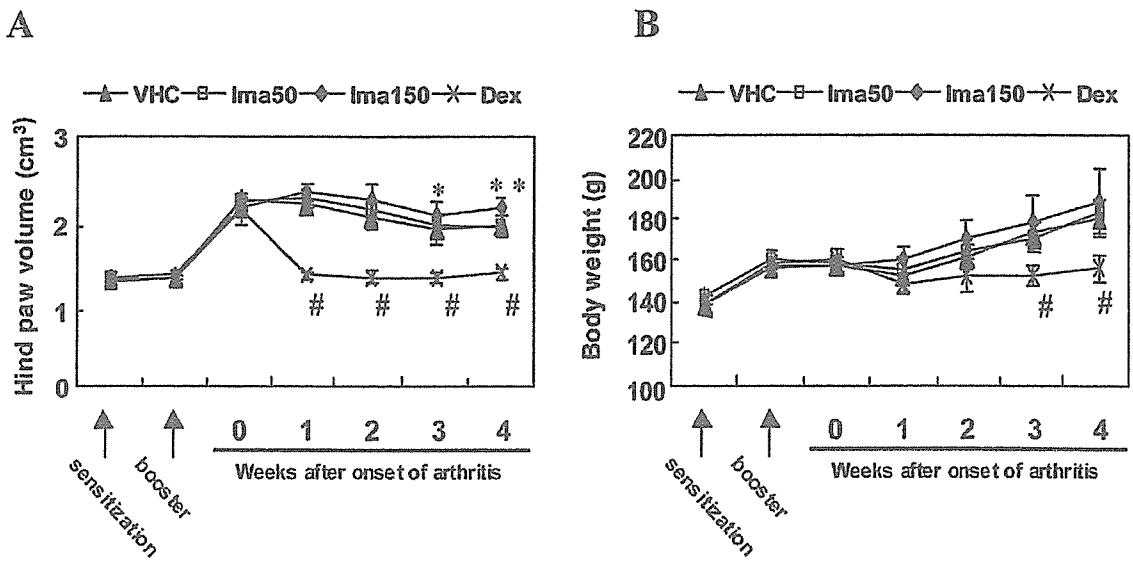

Fig. 1. Paw volume and body weight. Serial measurements of hind-paw volume (A) and body weight (B) in collagen-induced arthritis (CIA) rats administered with 50 mg/kg imatinib mesylate (*Ima50*; $n = 6$), 150 mg/kg imatinib mesylate (*Ima150*; $n = 6$), dexamethasone (*Dex*; $n = 5$), and vehicle (*VHC*; $n = 5$). $^{*}P < 0.05$; $^{**}P < 0.01$; $^{\#}P < 0.001$, compared with vehicle. *Bars* mean ± SD

Bio, Otsu, Japan) as described in the supplied protocol. M-CSF-dependent osteoclast precursors collected from bone marrow as described above or fresh adherent cells obtained from bone marrow cells of the same rats were seeded at a density of 5.0×10^3/wells in 96-well plates in medium with or without M-CSF, respectively. Imatinib mesylate was added to a final concentration of 0–4 μM as described in quadruplicate, and cells were incubated for 2 or 5 days. The cells were harvested with trypsin-EDTA and counted using a hemocytometer. In other wells, the cell proliferation reagent WST-1 (10 μl/well) was added at each time point and the cells were incubated for 2 h. Absorbance of the extracted products was measured at 440 nm using a Viento spectrophotometer (Dainippon, Osaka, Japan).

Statistical analysis

Data were statistically analyzed using an unpaired *t* test, the Mann–Whitney *U* test, and analysis of variance with Fisher's protected least significant difference test. StatView version 5.5 software performed statistical calculations (SAS Institute, Cary, NC, USA), and a *P* value of 0.05 indicated statistical significance.

Results

Effect of imatinib mesylate in CIA rats

The increased paw swelling induced in CIA rats was decreased by dexamethasone to the levels before clinical onset of arthritis. However, imatinib mesylate (50 or 150 mg/kg) could not reduce paw swelling (Fig. 1A). Moreover, the paws of rats given 150 mg/kg imatinib mesylate were more swollen than those of rats given vehicle at weeks 3 ($P = 0.011$) and 4 ($P = 0.005$).

The rats stopped growing at 3 weeks after sensitization, but growth resumed after the administration of either imatinib mesylate (50 or 150 mg/kg) or vehicle (Fig. 1B). In contrast, growth did not resume in CIA rats given dexamethasone. Gains in body weight during the last 2 weeks significantly differed between the groups given dexamethasone and the other three groups ($P < 0.001$).

Radiographic assessment

Radiographic examination showed that 150 mg/kg imatinib mesylate reduced destruction of the ankle and subtalar joints (Fig. 2A) and the MTP joints (Fig. 3A) at week 2. At week 4, radiographic destruction was reduced in the MTP joint but not in the ankle and subtalar joints. Imatinib mesylate at 50 mg/kg slightly inhibited destruction of the MTP joint at weeks 2 and 4, but not that of the ankle and subtalar joints. Dexamethasone almost completely prevented the destruction of both the MTP and the ankle and subtalar joints at weeks 2 and 4. The radiographic scores of the ankle and subtalar joint destruction (Fig. 2B) were significantly lower in rats given 150 mg/kg (1.50 ± 0.55) than 50 mg/kg (2.67 ± 0.52) of imatinib mesylate or vehicle (2.50 ± 0.55) at week 2 ($P = 0.010$ compared with vehicle). However, the three groups did not differ significantly at week 4. The mean radiographic scores of 0.20 ± 0.41 (week 2) and 1.08 ± 0.56 (week 4) for MTP joint destruction (Fig. 3B) in rats given 150 mg/kg imatinib mesylate were significantly lower than those of 1.45 ± 0.89 (week 2) and 2.18 ± 0.69

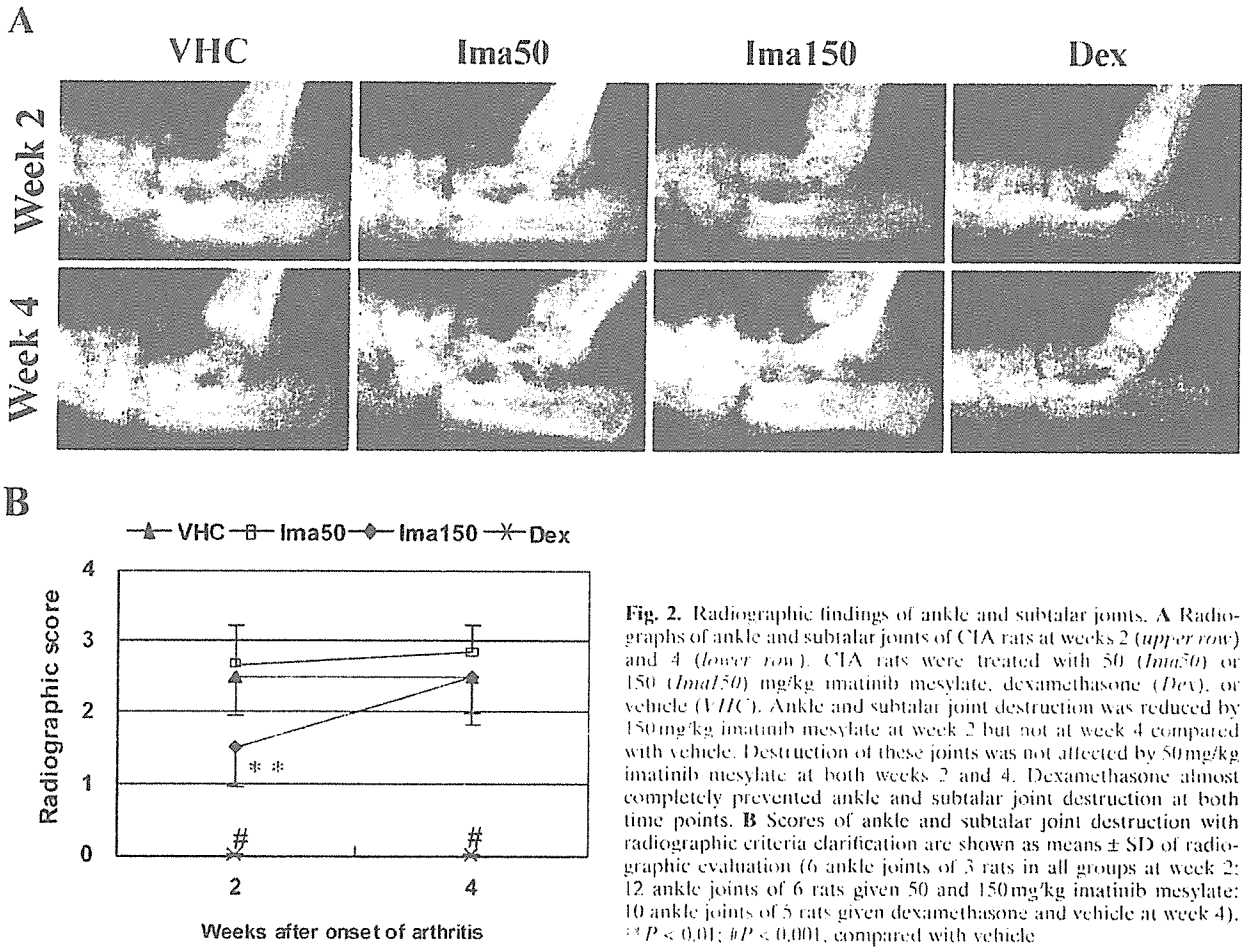

Fig. 2. Radiographic findings of ankle and subtalar joints. **A** Radiographs of ankle and subtalar joints of CIA rats at weeks 2 (*upper row*) and 4 (*lower row*). CIA rats were treated with 50 (*Ima50*) or 150 (*Ima150*) mg/kg imatinib mesylate, dexamethasone (*Dex*), or vehicle (*VHC*). Ankle and subtalar joint destruction was reduced by 150 mg/kg imatinib mesylate at week 2 but not at week 4 compared with vehicle. Destruction of these joints was not affected by 50 mg/kg imatinib mesylate at both weeks 2 and 4. Dexamethasone almost completely prevented ankle and subtalar joint destruction at both time points. **B** Scores of ankle and subtalar joint destruction with radiographic criteria clarification are shown as means ± SD of radiographic evaluation (6 ankle joints of 3 rats in all groups at week 2; 12 ankle joints of 6 rats given 50 and 150 mg/kg imatinib mesylate; 10 ankle joints of 5 rats given dexamethasone and vehicle at week 4). $^{**}P < 0.01$; $\#P < 0.001$, compared with vehicle

(week 4) in rats given vehicle ($P = 0.004$ and < 0.001 at weeks 2 and 4, respectively). The MTP joint destruction scores of 1.10 ± 0.55 and 1.80 ± 0.84 at weeks 2 and 4, respectively, in rats given 50 mg/kg imatinib mesylate were also lower than those of the control group given vehicle, but the differences did not reach statistical significance. The scores of the group treated with dexamethasone were 0.00 ± 0.00 and 0.04 ± 0.20 on the same respective days. These values from the groups treated with dexamethasone were significantly lower than those of the other groups ($P < 0.001$).

Histological assessment

Histological assessment revealed severe destruction in the MTP joints of rats given vehicle at week 2 (Fig. 4A). Synovitis, pannus formation, and articular cartilage and bone destruction with severe infiltration of neutrophils and lymphocytes characterized this lesion.

In the group given 150 mg/kg imatinib mesylate, less pannus had formed than in the group given vehicle at both weeks 2 and 4 (Fig. 4B), although synovitis developed at the joint space similarly to that in the group given vehicle. The number of TRAP-positive multinucleated cells (Fig. 4C) at the bone–pannus interface was significantly reduced in the group given 150 mg/kg imatinib mesylate (28.1 ± 14.9, $P = 0.028$) compared with that of the group given vehicle (77.0 ± 24.9). In the group given 50 mg/kg imatinib mesylate, although less pannus had formed at week 2, the amount formed at week 4 was identical to that of the group given vehicle, and the number of TRAP-positive multinucleated cells did not significantly differ (55.0 ± 20.8, $P = 0.245$). Synovitis, pannus formation, and joint destruction did not develop in the group given dexamethasone.

Imatinib mesylate inhibits proliferation of osteoclast precursors maintained by M-CSF

Imatinib mesylate dose-dependently inhibited the proliferation of osteoclast precursor cells in the presence of M-CSF (Fig. 5). After culture with imatinib mesylate for 2 days, the relative changes in the number of M-CSF-dependent osteoclast precursors (pre-OC) caused by 1 and 2 μM imatinib mesylate were 61.2% and 36.9%, respectively. On the other hand, those of fresh adherent bone marrow cells (BM cells) were 87.0% and 80.1%, respectively (Fig. 5A). The WST-1 assay revealed that the relative absorbance of pre-OC was reduced to 65.8% and 19.5% by 1 μM and 2 μM imatinib mesylate, respectively. In contrast,

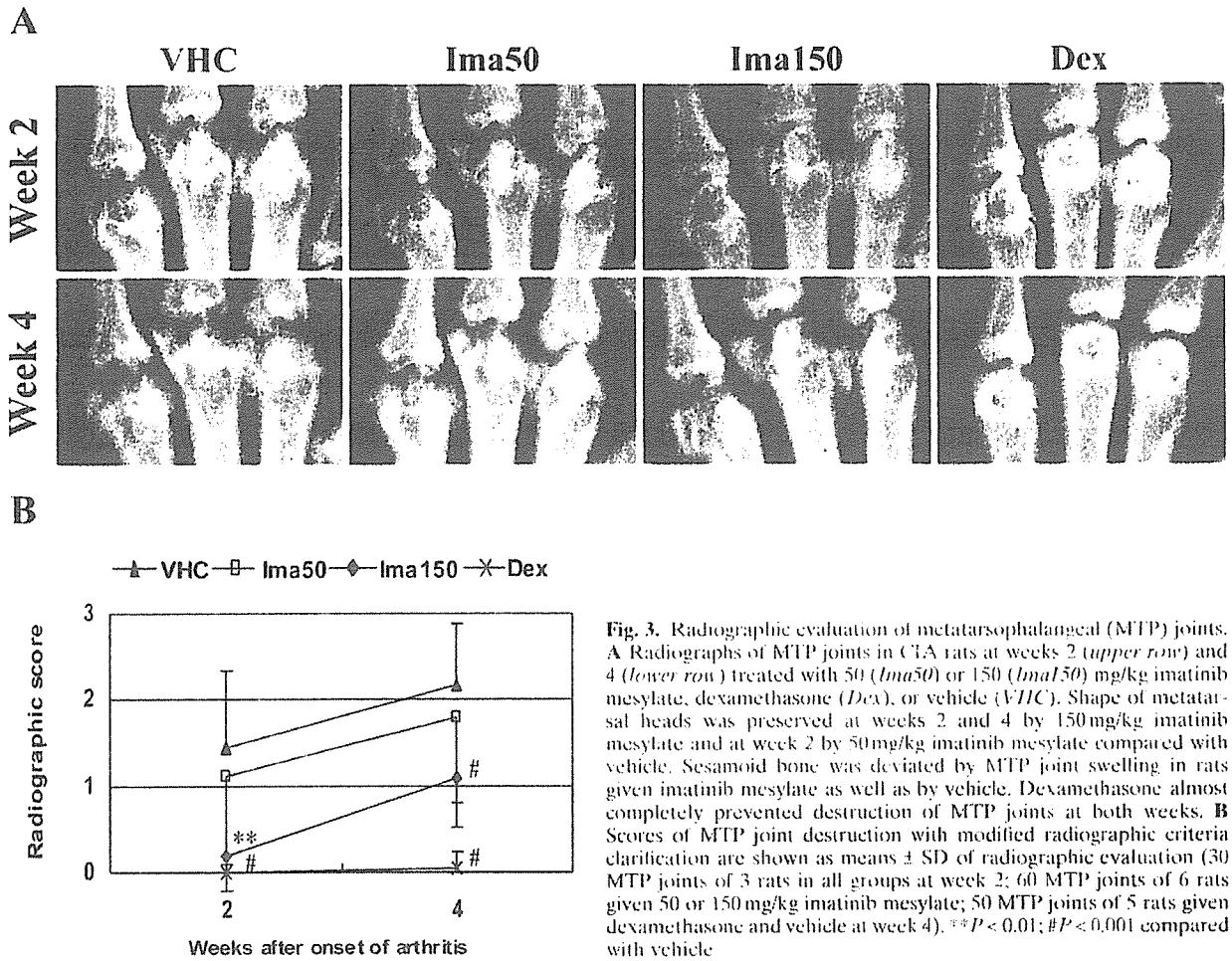

Fig. 3. Radiographic evaluation of metatarsophalangeal (MTP) joints. **A** Radiographs of MTP joints in CIA rats at weeks 2 (*upper row*) and 4 (*lower row*) treated with 50 (*Ima50*) or 150 (*Ima150*) mg/kg imatinib mesylate, dexamethasone (*Dex*), or vehicle (*VHC*). Shape of metatarsal heads was preserved at weeks 2 and 4 by 150 mg/kg imatinib mesylate and at week 2 by 50 mg/kg imatinib mesylate compared with vehicle. Sesamoid bone was deviated by MTP joint swelling in rats given imatinib mesylate as well as by vehicle. Dexamethasone almost completely prevented destruction of MTP joints at both weeks. **B** Scores of MTP joint destruction with modified radiographic criteria clarification are shown as means ± SD of radiographic evaluation (30 MTP joints of 3 rats in all groups at week 2; 60 MTP joints of 6 rats given 50 or 150 mg/kg imatinib mesylate; 50 MTP joints of 5 rats given dexamethasone and vehicle at week 4). $^{**}P < 0.01$; $^{\#}P < 0.001$ compared with vehicle

that of BM cells was reduced to 84.5% and 82.0% by 1 and 2 μM imatinib mesylate, respectively (Fig. 5B). After culture with imatinib mesylate for 5 days, the growth of M-CSF-dependent osteoclast precursors maintained with M-CSF was reduced to 20.5% by 1 μM and was abrogated by 2 μM imatinib mesylate (Fig. 5C).

Imatinib mesylate inhibits osteoclast formation

Imatinib mesylate dose-dependently inhibited osteoclast formation (Fig. 6A). The numbers of osteoclasts at day 5 were significantly reduced to 286.8 ± 59.8 ($P = 0.016$), 146.3 ± 75.1 ($P = 0.009$), and 5.5 ± 3.7 ($P < 0.001$) cells/48 wells after 5 days exposure to 0.25, 0.5, and 1 μM imatinib mesylate, respectively, compared with the nontreated group (403.5 ± 37.6 cells/48 wells). Cells did not change into TRAP-positive osteoclasts after exposure to concentrations of imatinib mesylate above 2 μM.

Imatinib mesylate does not influence osteoclastic bone resorption activity

Resorption areas in hydroxyapatite-coated slides after day 5 when osteoclasts had already differentiated were not reduced by imatinib mesylate. Resorption areas at day 10 with and without imatinib mesylate did not differ significantly (12.9% ± 6.2% and 13.1% ± 3.4%, respectively; see Fig. 6B).

Discussion

We are the first to reveal the positive effects of imatinib mesylate on joint destruction in arthritis model rats and a suppressive effect on osteoclastogenesis in vitro. Miyachi et al. [6] found that imatinib mesylate was therapeutically effective in a patient with RA. Eklund and Joensuu [7] also showed that imatinib mesylate was clinically effective in three patients with RA and postulated that one mechanism of action against arthritis is KIT receptor inhibition on mast cells. The present study found that imatinib mesylate alone

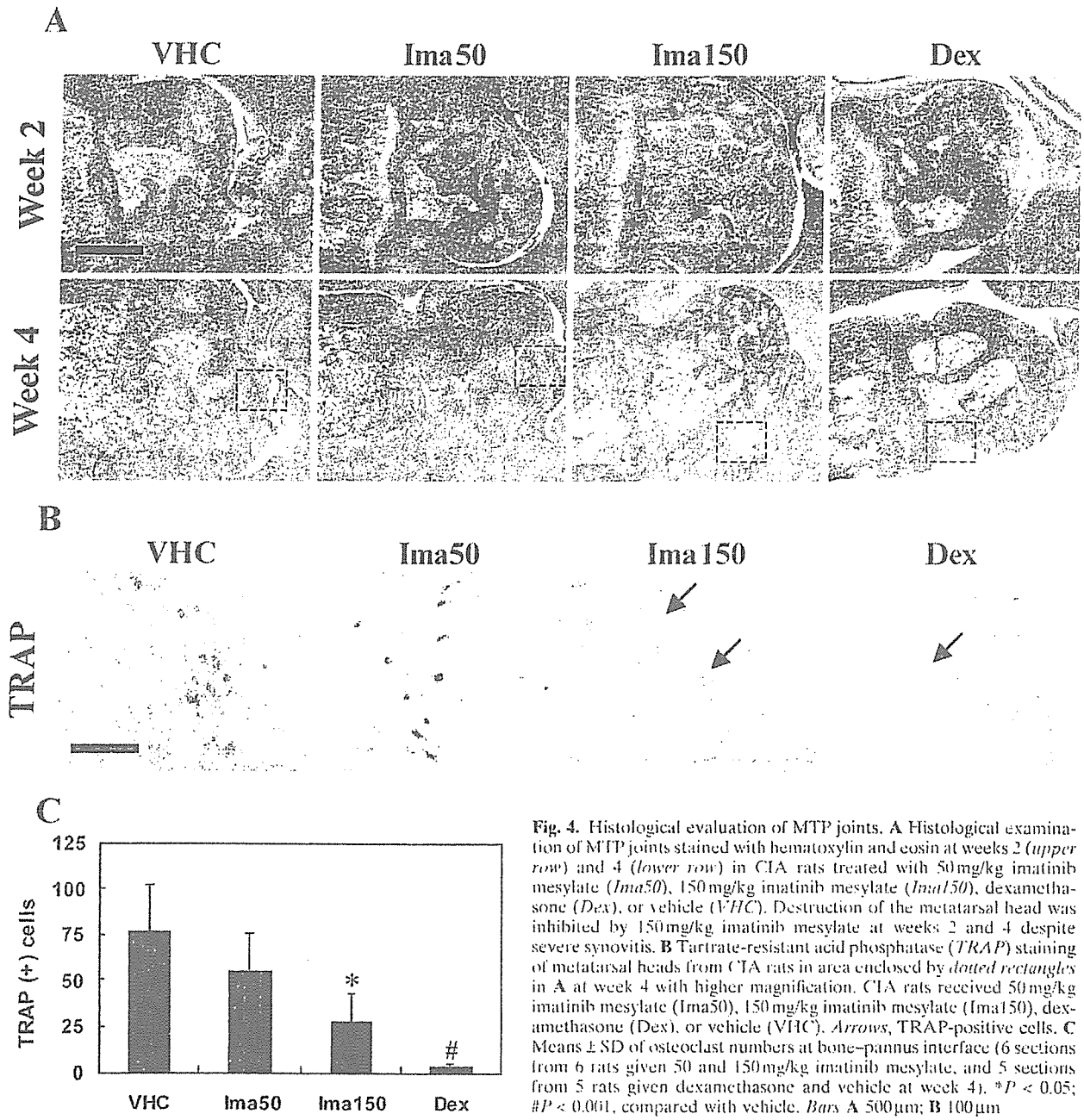

Fig. 4. Histological evaluation of MTP joints. **A** Histological examination of MTP joints stained with hematoxylin and eosin at weeks 2 (*upper row*) and 4 (*lower row*) in CIA rats treated with 50 mg/kg imatinib mesylate (*Ima50*), 150 mg/kg imatinib mesylate (*Ima150*), dexamethasone (*Dex*), or vehicle (*VHC*). Destruction of the metatarsal head was inhibited by 150 mg/kg imatinib mesylate at weeks 2 and 4 despite severe synovitis. **B** Tartrate-resistant acid phosphatase (*TRAP*) staining of metatarsal heads from CIA rats in area enclosed by *dotted rectangles* in **A** at week 4 with higher magnification. CIA rats received 50 mg/kg imatinib mesylate (Ima50), 150 mg/kg imatinib mesylate (Ima150), dexamethasone (Dex), or vehicle (VHC). *Arrows*, TRAP-positive cells. **C** Means ± SD of osteoclast numbers at bone–pannus interface (6 sections from 6 rats given 50 and 150 mg/kg imatinib mesylate, and 5 sections from 5 rats given dexamethasone and vehicle at week 4). $*P < 0.05$; $\#P < 0.001$, compared with vehicle. *Bars* **A** 500 μm; **B** 100 μm

did not improve inflammation in an animal model of RA but inhibited joint destruction and reduced the numbers of osteoclasts at the bone–pannus interface. This finding invokes the question of why imatinib mesylate was reasonably effective against clinical RA. All RA patients who were treated with imatinib mesylate in previous studies [6,7] received concomitant antiinflammatory drugs including glucocorticoids. However, the protective effect of glucocorticoids against joint destruction is not clear. Kirwan described that low-dose glucocorticoids administered for less than 2 years inhibits joint destruction [25], but Paulus et al. reported that glucocorticoid alone does not protect against joint destruction in RA patients [26]. Therefore, we speculated that the remarkable antirheumatic effects in the clinical setting reported by others [6,7] are the result of synergy between the antiinflammatory action of glucocorticoid and the antiosteoclastogenic effect of imatinib mesylate.

The cytokine M-CSF is essential for osteoclast formation [27]. We recently demonstrated that nurse-like cells established from RA synovium [28,29] secrete M-CSF, maintain osteoclast precursors for long periods, and might play an important role in the pathogenesis of joint destruction [20]. Imatinib mesylate is a tyrosine kinase inhibitor that inhibits *bcr-abl* expressed by CML progenitors, as well as PDGF and *c-kit*, which is a tyrosine kinase transmembrane

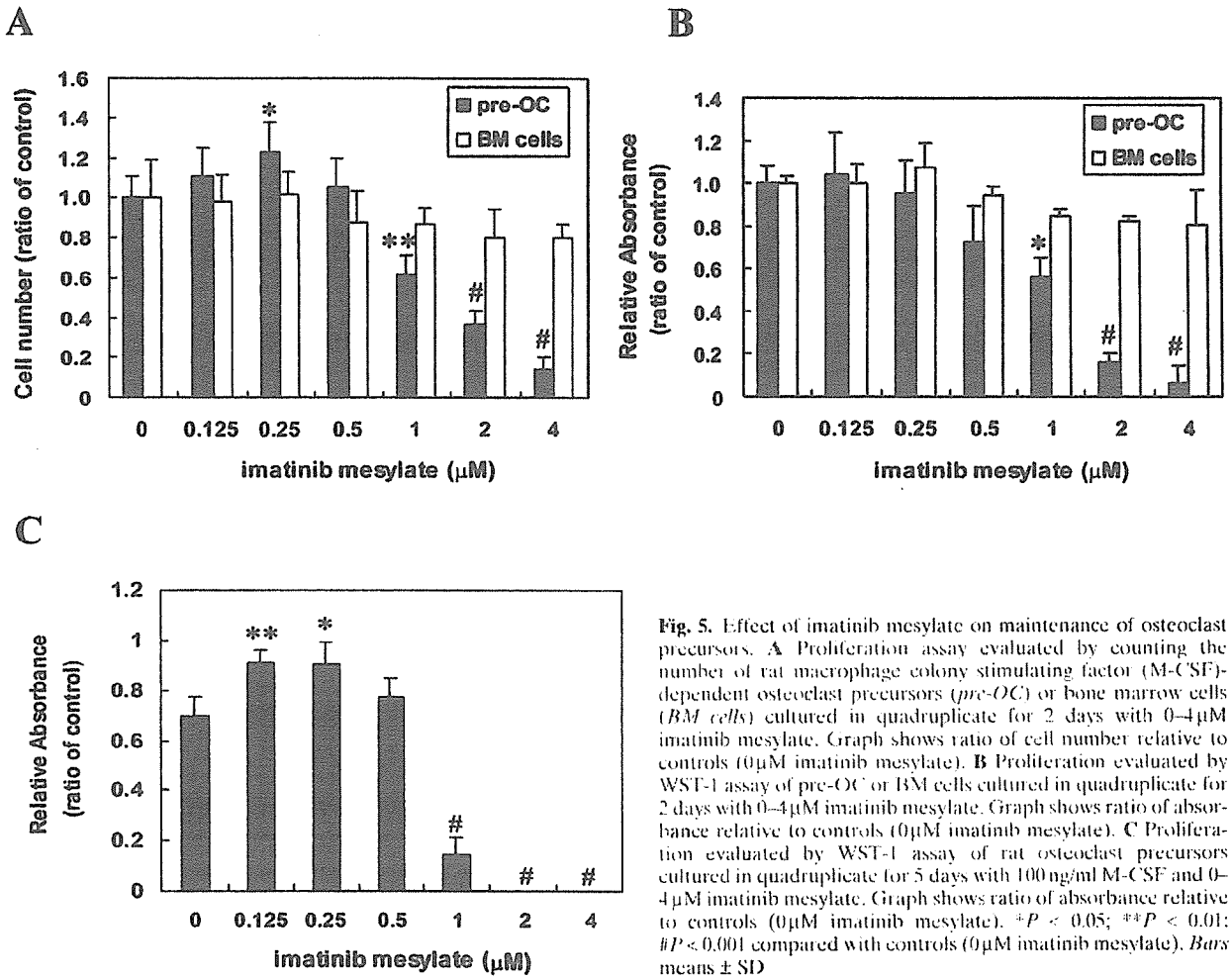

Fig. 5. Effect of imatinib mesylate on maintenance of osteoclast precursors. **A** Proliferation assay evaluated by counting the number of rat macrophage colony stimulating factor (M-CSF)-dependent osteoclast precursors (*pre-OC*) or bone marrow cells (*BM cells*) cultured in quadruplicate for 2 days with 0–4 μM imatinib mesylate. Graph shows ratio of cell number relative to controls (0 μM imatinib mesylate). **B** Proliferation evaluated by WST-1 assay of pre-OC or BM cells cultured in quadruplicate for 2 days with 0–4 μM imatinib mesylate. Graph shows ratio of absorbance relative to controls (0 μM imatinib mesylate). **C** Proliferation evaluated by WST-1 assay of rat osteoclast precursors cultured in quadruplicate for 5 days with 100 ng/ml M-CSF and 0–4 μM imatinib mesylate. Graph shows ratio of absorbance relative to controls (0 μM imatinib mesylate). $^{*}P < 0.05$; $^{**}P < 0.01$; $^{\#}P < 0.001$ compared with controls (0 μM imatinib mesylate). *Bars* means ± SD

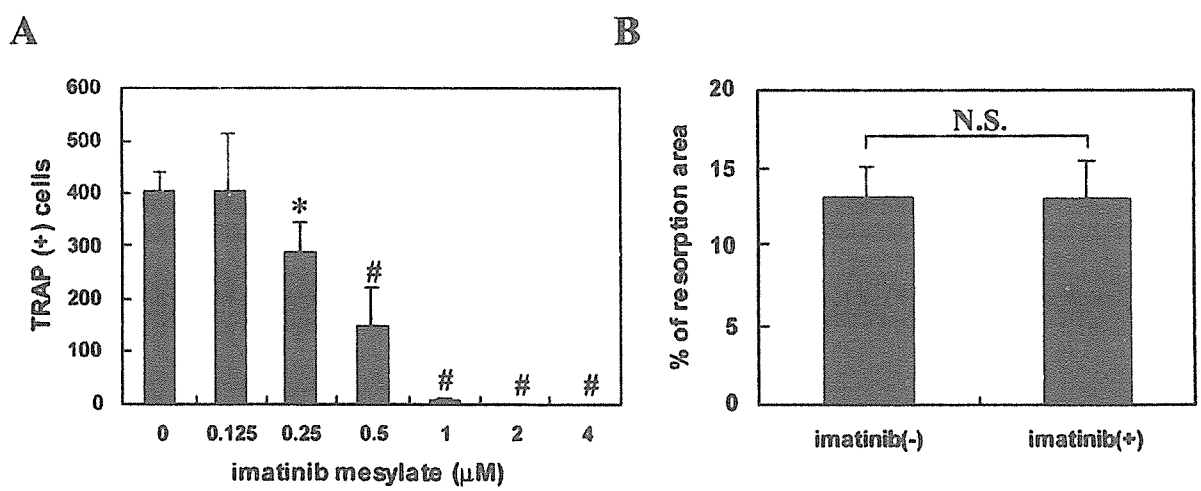

Fig. 6. Effect of imatinib mesylate on osteoclast differentiation and calcified matrix bone resorption by osteoclasts. **A** Numbers of TRAP-positive multinucleate cells (3 or more nuclei, $n = 4$; means ± SD) induced by 100 ng/ml M-CSF and 100 ng/ml soluble receptor activator of NF-κB ligand (sRANKL) together with 0–4 μM imatinib mesylate in quadruplicate. $^{*}P < 0.05$; $^{**}P < 0.01$; $^{\#}P < 0.001$ compared with 0 μM imatinib mesylate. **B** Ratio of resorption area to initial surface of hydroxyapatite-coated area at day 10 was not changed compared with that in quadruplicate cultures without imatinib mesylate. Imatinib mesylate (10 μM) was added to medium at day 5 when osteoclasts had differentiated. *N.S.*, not significant. *Bars* means ± SD

receptor that belongs to the FMS/PDGF receptor family of tyrosine protein kinases. Dewar et al. reported that imatinib mesylate inhibits the development of the monocyte/macrophage lineage from normal human bone marrow progenitors in vitro [30] and subsequently demonstrated that therapeutic concentrations of imatinib mesylate inhibit the phosphorylation of c-*fms* without downregulation of its expression [8]. These data suggest that imatinib mesylate inhibits the maintenance of osteoclast precursors by selectively blocking c-*fms* signaling and subsequently inhibits osteoclastogenesis in pannus as well as bone destruction in CIA rats.

However, this inhibitory effect on osteoclastogenesis and bone destruction was incomplete. Vascular endothelial growth factor (VEGF) as well as M-CSF plays a crucial role in the pathogenesis of inflammatory joint disease, including osteoclastogenesis [31]. Imatinib mesylate does not inhibit ligand-induced phosphorylation of VEGFR1 and VEGFR2 [32]. These findings might explain why osteoclastogenesis was not completely suppressed in vivo in our study. The partial suppression of osteoclastogenesis and the absence of a suppressive effect on the bone resorptive function of differentiated osteoclasts by imatinib mesylate might explain its incomplete suppressive effect on bone destruction.

Imatinib mesylate does not inhibit the tyrosine kinase, src [33,34], which is essential for osteoclast function [35]. Our finding that imatinib mesylate does not influence osteoclastic bone resorption activity is consistent with this fact.

The present study found that the ankle and subtalar joints were more damaged than the MTP joints. This difference might have resulted from the incomplete suppression of joint destruction and a difference in the mechanical stress loaded on these joints. The vertically loaded ankle and subtalar joints might be more susceptible to mechanical destruction than the nonvertically loaded MTP joints.

We found that dexamethasone suppressed synovitis and osteoclastogenesis in CIA rats, although dexamethasone increases osteoclast formation and lacunar resorption in the presence of M-CSF and RANKL in vitro [36]. On the other hand, dexamethasone suppresses the expression of activated NF-κB, which is involved in the inflammation process associated with adjuvant arthritis [37], and proliferating synoviocytes in pannus produce the factors essential for osteoclastogenesis such as M-CSF [20] and RANKL [38]. We therefore considered that the complete inhibition of synovitis with dexamethasone might result in the complete suppression of osteoclastogenesis.

In conclusion, imatinib mesylate prevents joint destruction in CIA rats by reducing osteoclastogenesis at the bone–pannus interface without affecting the inflammatory response. It also inhibited the proliferation of osteoclast precursors that results in a reduction of osteoclastogenesis in vitro. Imatinib mesylate inhibits osteoclastogenesis as well as joint destruction and therefore shows promise as a therapeutic agent against RA.

Acknowledgment Work was supported by grants from the Ministry of Health, Labour, and Welfare of Japan.

References

1. Goldring SR, Gravallese EM (2000) Pathogenesis of bone erosions in rheumatoid arthritis. Curr Opin Rheumatol 12:195–199
2. Druker BJ, Tamura S, Buchdunger E, Ohno S, Segal GM, et al. (1996) Effects of a selective inhibitor of the Abl tyrosine kinase on the growth of Bcr-Abl positive cells. Nat Med 2:561–566
3. Heinrich MC, Griffith DJ, Druker BJ, Wait CL, Ott KA, et al. (2000) Inhibition of c-kit receptor tyrosine kinase activity by STI 571, a selective tyrosine kinase inhibitor. Blood 96:925–932
4. Buchdunger E, Cioffi CL, Law N, Stover D, Ohno-Jones S, et al. (2000) Abl protein-tyrosine kinase inhibitor STI571 inhibits in vitro signal transduction mediated by c-kit and platelet-derived growth factor receptors. J Pharmacol Exp Ther 295:139–145
5. Tuveson DA, Willis NA, Jacks T, Griffin JD, Singer S, et al. (2001) STI571 inactivation of the gastrointestinal stromal tumor c-KIT oncoprotein: biological and clinical implications. Oncogene 20:5054–5058
6. Miyachi K, Ihara A, Hankins RW, Murai R, Maehiro S, et al. (2003) Efficacy of imatinib mesylate (STI571) treatment for a patient with rheumatoid arthritis developing chronic myelogenous leukemia. Clin Rheumatol 22:329–332
7. Eklund KK, Joensuu H (2003) Treatment of rheumatoid arthritis with imatinib mesylate: clinical improvement in three refractory cases. Ann Med 35:362–367
8. Dewar AL, Cambareri AC, Zannettino AC, Miller BL, Doherty KV, et al. (2005) Macrophage colony stimulating factor receptor, c-fms, is a novel target of imatinib. Blood 105:3127–3132
9. van de Wijngaert FP, Tas MC, Burger EH (1989) Conditioned medium of fetal mouse long bone rudiments stimulates the formation of osteoclast precursor-like cells from mouse bone marrow. Bone (NY) 10:61–68
10. Felix R, Cecchini MG, Hofstetter W, Elford PR, Stutzer A (1990) Impairment of macrophage colony-stimulating factor production and lack of resident bone marrow macrophages in the osteopetrotic op/op mouse. J Bone Miner Res 5:781–789
11. Kodama H, Yamasaki A, Nose M, Niida S, Ohgame Y, et al. (1991) Congenital osteoclast deficiency in osteopetrotic (op/op) mice is cured by injections of macrophage colony-stimulating factor. J Exp Med 173:269–272
12. Tanaka S, Takahashi N, Udagawa N, Tamura T, Akatsu T, et al. (1993) Macrophage colony-stimulating factor is indispensable for both proliferation and differentiation of osteoclast progenitors. J Clin Invest 91:257–263
13. Yasuda H, Shima N, Nakagawa N, Yamaguchi K, Kinosaki M, et al. (1998) Osteoclast differentiation factor is a ligand for osteoprotegerin /osteoclastogenesis-inhibitory factor and is identical to TRANCE/RANKL. Proc Natl Acad Sci U S A 95:3597–3602
14. Suda T, Takahashi N, Udagawa N, Jimi E, Gillespie MT, et al. (1999) Modulation of osteoclast differentiation and function by the new members of the tumor necrosis factor receptor and ligand families. Endocr Rev 20:345–357
15. Udagawa N, Takahashi N, Jimi E, Matsuzaki K, Tsurukai T, et al. (1999) Osteoblasts/stromal cells stimulate osteoclast activation through expression of osteoclast differentiation factor/RANKL but not macrophage colony-stimulating factor: receptor activator of NF-kappa B ligand. Bone (NY) 25:517–523
16. Wood DD, Ihrie EJ, Hamerman D (1985) Release of interleukin-1 from human synovial tissue in vitro. Arthritis Rheum 28:853–862
17. Guerne PA, Zuraw BL, Vaughan JH, Carson DA, Lotz M (1989) Synovium as a source of interleukin 6 in vitro. Contribution to local and systemic manifestations of arthritis. J Clin Invest 83:585–592
18. Ritchlin C (2000) Fibroblast biology. Effector signals released by the synovial fibroblast in arthritis. Arthritis Res 2:356–360
19. Takayanagi H, Iizuka H, Juji T, Nakagawa T, Yamamoto A, et al. (2000) Involvement of receptor activator of nuclear factor kappaB ligand/osteoclast differentiation factor in osteoclastogenesis from synoviocytes in rheumatoid arthritis. Arthritis Rheum 43:259–269
20. Tsuboi H, Udagawa N, Hashimoto J, Yoshikawa H, Takahashi N, et al. (2005) Nurse-like cells from patients with rheumatoid arthritis support the survival of osteoclast precursors via macrophage-colony stimulating factor production. Arthritis Rheum 52:3819–3828

21. Trentham DE, Townes AS, Kang AH (1977) Autoimmunity to type II collagen: an experimental model of arthritis. J Exp Med 146:857–868
22. Nishikawa M, Myoui A, Tomita T, Takahi K, Nampei A, et al. (2003) Prevention of the onset and progression of collagen-induced arthritis in rats by the potent p38 mitogen-activated protein kinase inhibitor FR167653. Arthritis Rheum 48:2670–2681
23. Cuzzocrea S, Mazzon E, Dugo L, Serraino I, Britti D, et al. (2001) Absence of endogeneous interleukin-10 enhances the evolution of murine type-II collagen-induced arthritis. Eur Cytokine Netw 12:568–580
24. Kobayashi K, Takahashi N, Jimi E, Udagawa N, Takami M, et al. (2000) Tumor necrosis factor alpha stimulates osteoclast differentiation by a mechanism independent of the ODF/RANKL-RANK interaction. J Exp Med 191:275–286
25. Kirwan JR (1995) The effect of glucocorticoids on joint destruction in rheumatoid arthritis. The Arthritis and Rheumatism Council Low-Dose Glucocorticoid Study Group. N Engl J Med 333:142–146
26. Paulus HE, Di Primeo D, Sanda M, Lynch JM, Schwartz BA, et al. (2000) Progression of radiographic joint erosion during low dose corticosteroid treatment of rheumatoid arthritis. J Rheumatol 27:1632–1637
27. Perkins SL, Kling SJ (1995) Local concentrations of macrophage colony-stimulating factor mediate osteoclastic differentiation. Am J Physiol 269:1024–1030
28. Takeuchi E, Tomita T, Toyosaki-Maeda T, Kaneko M, Takano H, et al. (1999) Establishment and characterization of nurse cell-like stromal cell lines from synovial tissues of patients with rheumatoid arthritis. Arthritis Rheum 42:221–228
29. Tomita T, Takeuchi E, Toyosaki-Maeda T, Oku H, Kaneko M, et al. (1999) Establishment of nurse-like stromal cells from bone marrow of patients with rheumatoid arthritis: indication of characteristic bone marrow microenvironment in patients with rheumatoid arthritis. Rheumatology (Oxf) 38:854–863
30. Dewar AL, Domaschenz RM, Doherty KV, Hughes TP, Lyons AB (2003) Imatinib inhibits the in vitro development of the monocyte/macrophage lineage from normal human bone marrow progenitors. Leukemia 17:1713–1721
31. Matsumoto Y, Tanaka K, Hirata G, Hanada M, Matsuda S, et al. (2002) Possible involvement of the vascular endothelial growth factor-Flt-1–focal adhesion kinase pathway in chemotaxis and the cell proliferation of osteoclast precursor cells in arthritic joints. J Immunol 168:5824–5831
32. Pietras K, Ostman A, Sjoquist M, Buchdunger E, Reed RK, et al. (2001) Inhibition of platelet-derived growth factor receptors reduces interstitial hypertension and increases transcapillary transport in tumors. Cancer Res 61:2929–2934
33. Buchdunger E, Cioffi CL, Law N, Stover D, Ohno-John S, et al. (2000) Abl protein-tyrosine kinase inhibitor STI571 inhibits in vitro signal transduction mediated by c-kit and platelet-sderived growth factor receptors. J Pharmacol Exp Ther 295:139–145
34. Schindler T, Bornmann W, Pellicena P, Miller WT, Clarkson B, et al. (2000) Structural mechanism for STI-571 inhibition of abelson tyrosine kinase. Science 289:1938–1942
35. Miyazaki T, Sanjay A, Neff L, Tanaka S, Horne WC, et al. (2004) Src kinase activity is essential for osteoclast function. J Biol Chem 279:17660–17666
36. Hirayama T, Danks L, Sabokbar A, Athanasou NA (2002) Osteoclast formation and activity in the pathogenesis of osteoporosis in rheumatoid arthritis. Rheumatology 41:1232–1239
37. Tsao PW, Suzuki T, Totsuka R, Murata T, Takagi T, et al. (1997) The effect of dexamethasone on the expression of activated NF-kappa B in adjuvant arthritis. Clin Immunol Immunopathol 83:173–178
38. Romas E, Bakharevski O, Hards DK, Kartsogiannis V, Quinn JM, et al. (2000) Expression of osteoclast differentiation factor at sites of bone erosion in collagen-induced arthritis. Arthritis Rheum 43:821–826

JOURNAL OF BONE AND MINERAL RESEARCH
Volume 21, Number 7, 2006
Published online on May 15, 2006; doi: 10.1359/JBMR.060411

Bone Morphogenetic Proteins in Bone Stimulate Osteoclasts and Osteoblasts During Bone Development

Mina Okamoto, Junko Murai, Hideki Yoshikawa, and Noriyuki Tsumaki

ABSTRACT: In this study, overexpression of noggin, a BMP antagonist, in developing bone caused significantly decreased osteoclast number as well as bone formation rate, resulting in increased bone mass with immature bone quality. BMP signaling plays important roles in normal bone development and regulation of bone resorption.

Introduction: Bone morphogenetic proteins (BMPs) act on various types of cells. Although involvement of BMP signals in osteoblast differentiation has been studied extensively, the effects of BMPs on osteoclasts have not been widely researched. Consequently, the net effects of BMPs on bone remain unclear. The purpose of this study was to delineate more fully the role of BMPs in skeletal biology.
Materials and Methods: We generated transgenic mice that express BMP4 or noggin in bone under the control of the 2.3-kb α1(I) collagen chain gene (*Col1a1*) promoter, and analyzed their bone phenotype. We also analyzed bone of transgenic mice expressing BMP4 specifically in cartilage.
Results: Mice overexpressing BMP4 in bone developed severe osteopenia with increased osteoclast number. Mice overexpressing noggin, a BMP antagonist, in bone showed increased bone volume associated with decreased bone formation rate and decreased osteoclast number. The noggin-transgenic tibias exhibited reduced periosteal bone formation and reduced resorption of immature bone in marrow spaces, associated with frequent fractures at the diaphysis. Co-culture of primary osteoblasts prepared from noggin-transgenic calvariae and wildtype spleen cells resulted in poor osteoclast formation, which was rescued by addition of recombinant BMP2, suggesting that noggin inhibits osteoclast formation by attenuating BMP activities in noggin-transgenic mice. The expression levels of *Rankl* were not decreased in primary osteoblasts from noggin transgenic mice. Immunoblot analysis showed increased phosphorylation of Smad1/5/8 in osteoclast precursor cells after 20-minute treatment with BMPs, suggesting that these cells are stimulated by BMPs. Mice overexpressing BMP4 in cartilage had enlarged bones containing thick trabeculae, possibly because of expansion of cartilage anlagen.
Conclusions: Overexpression of noggin in bone revealed that BMP signals regulate bone development through stimulation of osteoblasts and osteoclasts.
J Bone Miner Res 2006;21:1022–1033. Published online on May 15, 2006; doi: 10.1359/JBMR.060411

Key words: bone morphogenetic proteins, noggin, osteoclasts, endochondral bone formation, transgenic mice

INTRODUCTION

BONE MORPHOGENETIC PROTEINS (BMPs) were originally identified as secreted substances capable of inducing ectopic formation of cartilage and bone when implanted subcutaneously or in muscle pouches.[1] Subsequent molecular cloning studies have revealed that BMPs comprise a large subfamily of the TGF-β superfamily.[2] BMPs bind to BMP receptor types I and II, and their signal is mediated by phosphorylation of receptor-regulated Smads (R-Smads) such as Smads 1, 5, and 8.[3] Phosphorylated R-Smads form heteromers with Smad4, which is a common-partner Smad (Co-Smad), and the heteromers translocate into the nucleus. BMP signaling is delicately regulated at multiple levels: extracellularly, at the membrane site, and intracellularly.[4] In the extracellular space, several molecules antagonize BMPs. One of those antagonists is noggin, which binds to BMPs 2, 4, and 7 and prevents them from interacting with their receptors.[4,5] Recent studies of co-crystal structure clearly show that noggin very specifically inhibits BMPs.[6] Noggin has been used to block BMP action and study its role in certain tissues.

Limb bones are formed through a process called endochondral bone formation. During this process, mesenchymal cells first differentiate into chondrocytes, which form the cartilage anlagen of the bones. Then, the central region of each cartilage anlage is invaded by blood vessels, osteoblasts, osteoclasts, and hematopoietic cells, resulting in for-

The authors state that they have no conflicts of interest.

Department of Orthopaedic Surgery, Osaka University Graduate School of Medicine, Suita, Osaka, Japan.

mation of primary ossification centers. Bone gradually replaces the cartilage. Osteoblasts form woven bone on the remnant of the calcified cartilage matrix, modeling the trabeculae of the primary spongiosa. Trabecular bone then undergoes remodeling consisting of resorption by osteoclasts and apposition of newly formed bone matrix by osteoblasts, creating secondary spongiosa.[7] Bone remodeling continues in postnatal life to maintain bone mass. Osteoblasts develop from mesenchymal cells, whereas osteoclasts develop from hematopoietic cells of the monocyte/macrophage lineage. Osteoclastic bone resorption and osteoblastic bone formation are coupled on the surface of trabeculae of secondary spongiosa. Osteoblasts and stromal cells regulate osteoclast differentiation by producing RANKL (which supports osteoclast differentiation) and osteoprotegerin (OPG; which inhibits RANKL function by competing with RANK for RANKL).[8]

Conventional gene knockout experiments have shown that BMPs have diverse biological activities during early embryogenesis and various aspects of organogenesis, mediated by their ability to regulate proliferation, differentiation, and apoptosis of various types of cells.[9] Recent osteoblast-specific downregulations of BMP signals in mice have clarified the role of BMPs in osteoblast differentiation. In 4-week-old to 6-month-old mice, osteoblast-specific expression of dominant-negative BMP receptor type IB[10] and osteoblast-specific gene ablation of BMP receptor type IA[11] cause inhibition of osteoblast differentiation and a decrease in bone volume but do not change the osteoclast number, indicating that BMP signals are important for maintenance of bone mass by osteoblasts in postnatal life. In 10-month-old mice, osteoblast-specific gene ablation of BMP receptor type IA causes a decrease in osteoclastic bone resorption activity. Such findings have led to speculation that loss of BMP signaling in osteoblasts leads to impairment of osteoclast-supporting activities, causing downregulation of osteoclast function as the mice age.[11] In mice older than 4 weeks, overexpression of noggin in mature osteoblasts under the control of the osteocalcin promoter sequence causes osteopenia (bone loss) and reduction of the bone formation rate, but does not change the osteoclast number.[12] Thus, BMP signals are important for osteoblast differentiation and function.

On the other hand, several reports indicate that osteoclasts express BMP receptors and that BMPs directly stimulate osteoclast differentiation in vitro.[13–15] Osteoclast differentiation supported by macrophage colony-stimulating factor (M-CSF) and RANKL is enhanced in the presence of BMPs. However, there have been no reported studies of the effects of BMPs on osteoclasts during bone formation in vivo. The process of endochondral bone formation during skeletogenesis is recapitulated in fracture repair.[16,17] BMPs have been clinically used to promote healing of fractures.[18–20] Further clarification of effects of BMPs in bone is needed to improve our understanding of skeletal biology and improve the efficacy of BMPs in bone repair.

The aim of this study was to examine more fully roles of BMPs in skeletal biology. We generated transgenic mice overexpressing BMP4 or noggin under the control of the bone-specific 2.3-kb α1(I) collagen chain gene (*Col1a1*) promoter sequence. Transcriptional activity of the *Col1a1* promoter in osteoblasts is much stronger than that of the osteocalcin promoter.[21] Also, we examined bones of mice with cartilage-specific overexpression of BMP4 to assess the stage-specific effects of BMP4 on endochondral bone formation.

MATERIALS AND METHODS

Generation of transgenic mice

The *Col1a1-LacZ*, *Col1a1-noggin,* and *Col1a1-Bmp4* transgene constructs were created by replacing the *Col11a2* promoter sequence of the *Col11a2-LacZ, Col11a2-noggin,* and *Col11a2-Bmp4* transgene constructs,[22] respectively, with the 2.3-kb *Col1a1* promoter sequence.[23] The plasmids were digested to release the inserts from the vector backbone and the *Col11a2* enhancer sequences. The *Col11a2-Bmp4* insert was prepared as described previously.[22] Transgenic mice were produced by microinjecting each of the inserts into the pronuclei of fertilized eggs from F1 hybrid mice (C57BL/6 × DBA) as described previously.[24] Wildtype littermates were used as controls. All present animal experiments were approved by the institutional review board of Osaka University Graduate School of Medicine.

Real-time RT-PCR analysis

Total RNA was extracted from various tissues of 3-week-old mice and primary osteoblasts using Isogen (Wako Pure Chemical Co., Osaka, Japan). The RNA was digested with DNase to eliminate any contaminating genomic DNA before real-time quantitative RT-PCR. RNA samples were further purified using RNeasy Mini Kits (Qiagen, Santa Clarita, CA, USA). Real-time RT-PCR was performed as described previously.[25] The primer pair for noggin was as follows: up, 5′-CGGCCAGCACTATCTACACA-3′; down, 5′-GCGTCTCGTTCAGATCCTTC-3′. The product size for noggin was 116 bp. Primer pairs for *Rankl* and *Opg* were prepared using previously reported methods.[26] The quantified individual RNA expression levels were normalized to the respective tubulin expression levels.

μCT analysis

The tibias were dissected and scanned using a microfocus X-ray CT system (SMX-100CT-SV; Shimadzu, Kyoto, Japan). The proximal metaphyseal region and the diaphyseal region where the fibula attaches to the tibia were scanned at the following resolutions: 2.4 μm for 17.5 days postcoitum (d.p.c.) tibia; 3.3 μm for 2-week-old tibia; 10.7 μm for 3-week-old tibia; 10.6 μm for 8-week-old tibia. The data were reconstructed to produce images of the tibia, using 3D visualization and measurement software (Vay Tek).

Histological analysis and histomorphometry

Mice were dissected using a stereomicroscope, and tissue samples were fixed in 4% paraformaldehyde and dehydrated. Samples from mice older than 0 days were decalcified. Samples were processed, embedded in paraffin, and sectioned. Each serial section was stained using one of the

following procedures: H&E staining; the von Kossa reaction; or TRACP staining, using a TRACP staining kit (Hokudo). Immunohistochemistry and in situ hybridization were performed as previously described.[25] Dynamic histomorphometric indices were determined by double fluorescence labeling in tibias and vertebral bodies. Three-week-old wildtype and transgenic mice were administered tetracycline (20 mg/kg body weight, IP; Sigma-Aldrich), followed 2 days later by administration of a calcein label (10 mg/kg body weight; Wako). At 48 h after calcein administration, the mice were killed. Bones were fixed with ethanol, embedded in methylmethacrylate, and sectioned. Sections were examined using a fluorescence microscope. The histomorphometric analyses were performed by staff at the Niigata Bone Science Institute (Niigata, Japan).

Osteoblast and osteoclast culture

Primary osteoblasts were isolated from calvariae of neonatal mice, using previously described methods.[27] Co-culture experiments were performed using previously described methods.[28] Briefly, primary osteoblasts (1×10^4 cells/cm^2) prepared from wildtype or *Col1a1-noggin* transgenic mice were co-cultured with spleen cells (5×10^5 cells/cm^2) prepared from wildtype mice in α-MEM containing 10% FCS and 10^{-8} M 1α,25(OH)$_2$D$_3$-dihydroxyvitamin D$_3$ in 48-well plates. Co-cultures containing transgenic osteoblasts were also performed in the presence of recombinant human BMP2 proteins (rhBMP2; AstellasPharma) at various concentrations. Osteoclast differentiation was evaluated by TRACP staining. Multinucleated TRACP$^+$ cells with more than three nuclei were counted under a microscope. To test resorption activity, co-cultures were performed on 16-well hydroxyapatite-coated slides (Osteologic; Becton Dickinson) for 14 days, and the resorption area was calculated by computer-assisted image analysis. Primary osteoblasts were cultured for 3 days in α-MEM containing 10% FCS and 10^{-8} M 1α,25(OH)$_2$D$_3$ in the absence or presence of various concentration of rhBMP2, followed by analysis of *Rankl/Opg* expression of the osteoblasts by real-time RT-PCR.

Smad pathways in macrophages

Nearly pure macrophages were prepared from mouse bone marrow cultures treated with M-CSF, using previously described methods.[14] Macrophages were incubated for 20 minutes in the presence or absence of rhBMP2 at various concentrations. The macrophages were lysed and subjected to Western blotting using a rabbit polyclonal antibody against phospho-Smad1/5/8 (Cell Signaling Technology) and an anti-Smad 1 antibody (Calbiochem).

Statistical analysis

Results are expressed as mean ± SD. The unpaired *t*-test was used to compare data between wildtype and transgenic mice. A p value of <0.05 was considered to indicate significance.

RESULTS

Overexpression of BMP4 in bone caused severe bone loss associated with increased osteoclast number during endochondral bone development

When ligated to the *LacZ* reporter gene, the 2.3-kb *Col1a1* promoter sequence directed expression specifically to bone at birth (Figs. 1A and 1B), as previously reported.[23] The pattern of *LacZ* expression indicated by X-gal staining was specific to ossification centers of skeletal components in limbs, rib bones, and calvariae. *LacZ* was not expressed in cartilage or other tissues. We prepared the *Col1a1-Bmp4* transgene by ligating the promoter sequence to the *Bmp4* cDNA (Fig. 1C) and injected the construct to pronuclei of ova. The *Col1a1-Bmp4* transgenic mice died shortly after birth, probably because of impaired locomotion caused by fragility of bones. We obtained five transgenic founder embryos that exhibited similar obvious abnormalities. X-ray photographs taken 18.5 d.p.c. showed irregularly shaped bones in *Col1a1-Bmp4* transgenic embryos (Fig. 1D). Bones, including the humeri and femora, of transgenic mice were more radiolucent than the wildtype. Alcian blue and alizarin red staining showed deformity of bones including humeri (Figs. 1E and 1F). μCT analysis revealed osteopenia (loss of bone) in the ossification center of humeri of *Col1a1-Bmp4* transgenic mice (Fig. 1H) compared with the wildtype (Fig. 1G). Trabecular bone was almost completely absent from the marrow cavities of transgenic mice (Fig. 1H).

Histological analysis (von Kossa staining of semiserial sections of H&E-stained sections [Figs. 2A and 2B]) of proximal humeri at 18.5 d.p.c. showed reduced calcification in ossification centers of *Col1a1-Bmp4* transgenic mice (Fig. 2D) compared with the wildtype (Fig. 2C). Magnified images of bone marrow cavities showed absence of bony matrix in *Col1a1-Bmp4* transgenic mice (Fig. 2F), whereas solid bone matrix was clearly present in the wildtype (Fig. 2E). When the semiserial sections were immunostained using anti-phospho-Smad1/5/8, cells in bone marrow cavities of *Col1a1-Bmp4* transgenic mice (Fig. 2H) exhibited greater immunoreactivity than their wildtype counterparts (Fig. 2G), suggesting that BMP signals were overactivated in bone marrow of transgenic mice. There were many TRACP$^+$ osteoclasts in bone marrow cavities of *Col1a1-Bmp4* transgenic mice (Fig. 2J) compared with the wildtype (Fig. 2I). Because the *Col1a1-Bmp4* transgenic mice had markedly lower bone surface area than the wildtype, the number of TRACP$^+$ cells per bone surface area was markedly greater in the transgenic mice. These results suggest that BMP4 overexpression in bone of *Col1a1-Bmp4* transgenic mice caused osteopenia associated with enhanced Smad phosphorylation in various cells and increased number of TRACP$^+$ cells in bone marrow cavities.

Col1a1-noggin transgenic mice exhibited increased bone volume associated with decreased osteoclast number from embryonic stage

Figure 3A shows the procedure in which the *Col1a1-noggin* transgene was constructed by ligating the 2.3-kb

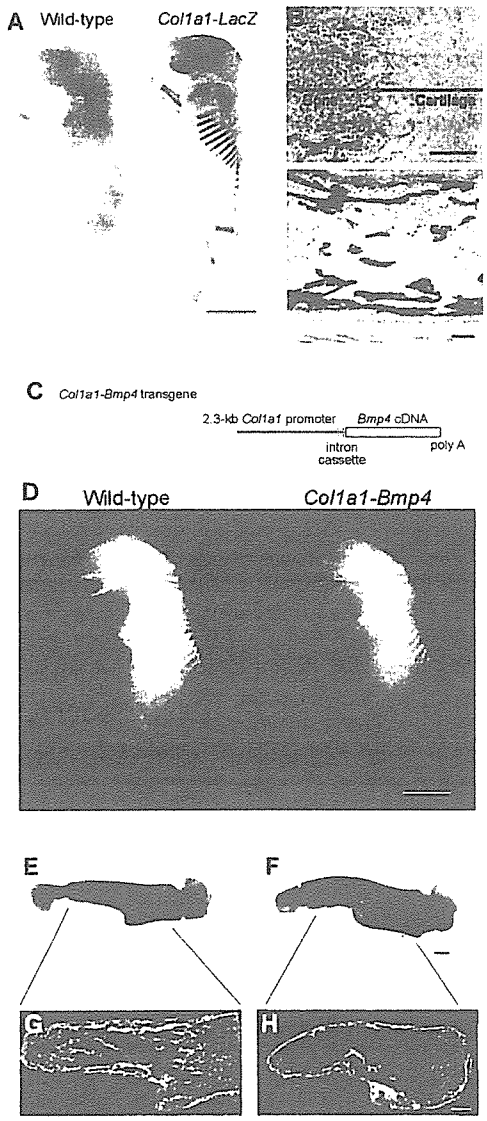

FIG. 1. Osteopenia in *Col1a1-Bmp4* transgenic mice. (A) X-gal staining of wildtype and *Col1a1-LacZ* transgenic mice at birth. The 2.3-kb *Col1a1* promoter sequence directed *LacZ* reporter gene expression specifically in bone. Scale bar, 2 mm. (B) Sagittal sections of *Col1a1-LacZ* transgenic tibias stained with X-gal. Note the X-gal staining in osteoblasts on the trabecular bone in distal metaphysis (top) and osteoblasts around cortical bone in diaphysis (bottom). No X-gal staining in chondrocytes (top). Counterstained with eosin. Scale bars, 100 μm. (C) Schematic representation of *Col1a1-Bmp4* transgene construct. (D) X-ray photograph of wildtype embryo (left) and *Col1a1-Bmp4* transgenic embryo (right) at 18.5 days postcoitum (d.p.c.). Bones of *Col1a1-Bmp4* transgenic embryo were irregular and radiolucent. Scale bars, 2 mm. (E and F) Alcian blue and alizarin red staining of humerus from (E) wildtype embryo and (F) *Col1a1-Bmp4* transgenic embryo at 18.5 d.p.c. Scale bar, 200 μm. (G and H) μCT images of ossification center of humerus of (G) wildtype and (H) *Col1a1-Bmp4* transgenic mice at 18.5 d.p.c. Reconstructed sagittal views. Scale bar, 200 μm.

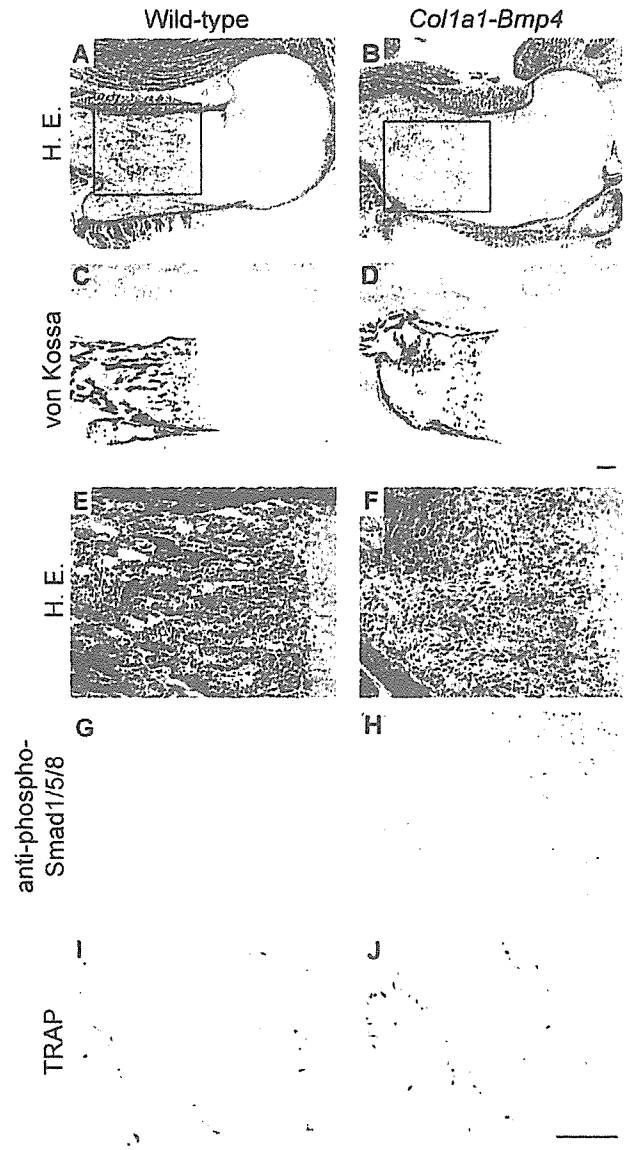

FIG. 2. Histological analysis of proximal humerus of *Col1a1-Bmp4* transgenic mice at 18.5 d.p.c. (A, C, E, G, and I) Wildtype mice and (B, D, F, H, and J) *Col1a1-Bmp4* transgenic mice. (A and B) H&E staining. Semiserial sagittal sections of A and B, stained using von Kossa method, are shown in C and D, respectively. Magnification of boxed regions in A and B are shown in E and F, respectively. Semiserial sagittal sections of E and F, immunostained using anti-phospho-Smad1/5/8 antibody, are shown in G and H, respectively. This antibody recognizes only phosphorylated forms of Smad1/5/8. Semiserial sections of E and F, stained for TRACP, are shown in I and J, respectively. Scale bar, 200 μm.

Col1a1 promoter to noggin cDNA. *Col1a1-noggin* transgenic mice were viable and fertile, and 2 *Col1a1-noggin* transgenic lines were established. The phenotypes of the two transgenic lines were similar, and one line was subjected to close examination. Until 1 week after birth, *Col1a1-noggin* transgenic mice were not visibly distinguishable from the wildtype. Staining of skeletal components of transgenic embryos with Alcian blue at various stages showed that the shapes and sizes of primordial cartilage were normal (data not shown). One week after birth, transgenic mice began to develop dwarfism, which was clearly evident in 3-week-old mice (Fig. 3B). X-ray photographs showed that *Col1a1-noggin* transgenic mice had thicker tra-

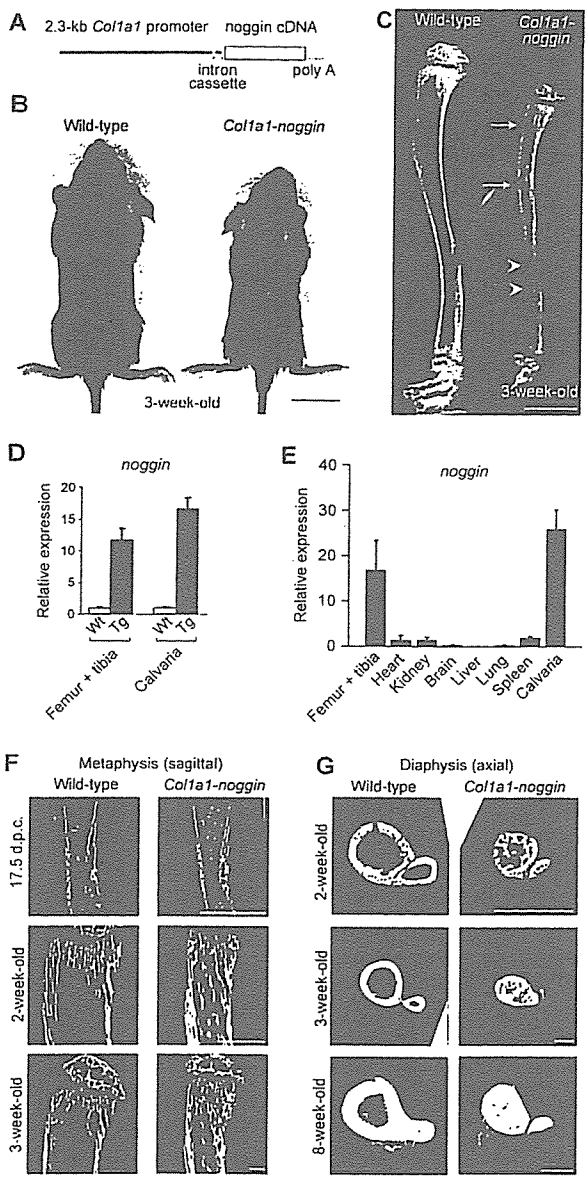

FIG. 3. Phenotype and noggin expression in *Col1a1-noggin* transgenic mice. (A) Schematic representation of the *Col1a1-noggin* transgene construct. (B) Three-week-old wildtype and *Col1a1-noggin* transgenic mice. Transgenic mice developed postnatal dwarfism. Scale bar, 1 cm. (C) X-ray image of the tibia at 3 weeks of age. Note thick trabecular (arrows) and cortical (arrowheads) bone in *Col1a1-noggin* transgenic mice, compared with wildtype mice. Scale bar, 2 mm. (D) Relative expression levels of noggin mRNA in total femur + tibia and in calvaria at 3 weeks of age, measured by real-time RT-PCR. Real-time RT-PCR was performed three times. Data are presented as mean ± SD. Wt, wildtype mice; Tg, *Col1a1-noggin* transgenic mice. The wildtype expression level was designated as 1. (E) Relative expression levels of noggin mRNA in various tissues from 3-week-old *Col1a1-noggin* transgenic mice, measured by real-time RT-PCR. RT-PCR was performed three times. Data are presented as mean ± SD. (F) μCT images of proximal metaphysis of tibia of wildtype and *Col1a1-noggin* transgenic mice at 17.5 d.p.c., 2 weeks of age, and 3 weeks of age. Sagittal views were reconstructed. Scale bar, 500 μm. (G) Axial views of μCT images of distal one third of diaphysis of tibia associated with fibula of wildtype and *Col1a1-noggin* transgenic mice at 2, 3, and 8 weeks of age. Scale bar, 500 μm.

becular bone and cortex than the wildtype, especially in tibias (Fig. 3C). Real-time RT-PCR using total RNA extracted from femur + tibia or calvaria showed that *Col1a1-noggin* transgenic mice had much higher expression levels of noggin mRNA than the wildtype (Fig. 3D). It seems that the *Col1a1-noggin* transgene was expressed at much higher levels in bone (femur + tibia or calvaria) than in other tissues (Fig. 3E). μCT analysis revealed that from the embryonic stage (17.5 d.p.c.) to 3 weeks after birth, the tibias of *Col1a1-noggin* transgenic mice (Fig. 3F) had a greater volume of trabecular bone than the wildtype. In the diaphyseal region of transgenic tibias, marrow cavities progressively filled with cortical bone from 2 to 8 weeks of age (Fig. 3G).

In histological analysis of primary ossification centers of tibias, there was no marked difference in the number of osteoblasts expressing *Col1a1* mRNA (a marker of osteoblasts) between *Col1a1-noggin* transgenic mice and wildtype mice, whereas there were fewer $TRACP^+$ osteoclasts in transgenic mice than in wildtype mice at 17.5 d.p.c. (Fig. 4A). In the primary ossification centers of tibias at birth and the proximal metaphyseal region of tibias at 3 weeks after birth, the number of $TRACP^+$ cells was lower in transgenic mice than in wildtype mice (Figs. 4B and 4C). At the diaphysis of growing long bones, an increase in diameter is the result of deposition of new bone at the outer (periosteal) surface and is accompanied by enlargement of the marrow cavity caused by resorption exceeding formation at the inner (endosteal) surface. In wildtype mice, $TRACP^+$ osteoclasts were located at the inner surface of the cortex, whereas no $TRACP^+$ cells were observed in transgenic mice (Fig. 4D). These results suggest that overexpression of noggin under the control of *Col1a1* promoter in developing bone causes thickening of trabecular bone and elimination of marrow cavities in cortical bone, associated with a reduced number of osteoclasts.

Col1a1-noggin transgenic mice exhibited increased bone volume, reduced bone formation rate, and reduced osteoclastic bone resorption

Figure 5 shows the results of bone histomorphometric assays. At the metaphyseal region of the proximal tibia at 3 weeks of age, trabecular bone volume was significantly greater in *Col1a1-noggin* transgenic mice than in wildtype mice (Fig. 5A). The osteoblast number (osteoblast surface area per bone surface area) was greater in transgenic mice than in wildtype mice (Fig. 5B). Significantly increased trabecular bone volume/tissue volume was also noted in lumbar vertebral bodies of *Col1a1-noggin* transgenic mice at 3 weeks of age (10.2 ± 2.9% in wildtype and 13.6 ± 4.7% in *Col1a1-noggin* transgenic mice, $n = 6$, $p = 0.01$). We analyzed dynamic changes in bone remodeling by injecting tetracycline and calcein at 2-day intervals. Vertebral bodies were subjected to dynamic analysis because of their sufficient areas of spongiosa for analysis at 3 weeks of age. The distance between the two consecutive labels in lumbar vertebral bodies was significantly less in transgenic mice (Fig. 5D), as indicated by a decreased mineral apposition rate (Fig. 5C), compared with wildtype mice. There was no sig-

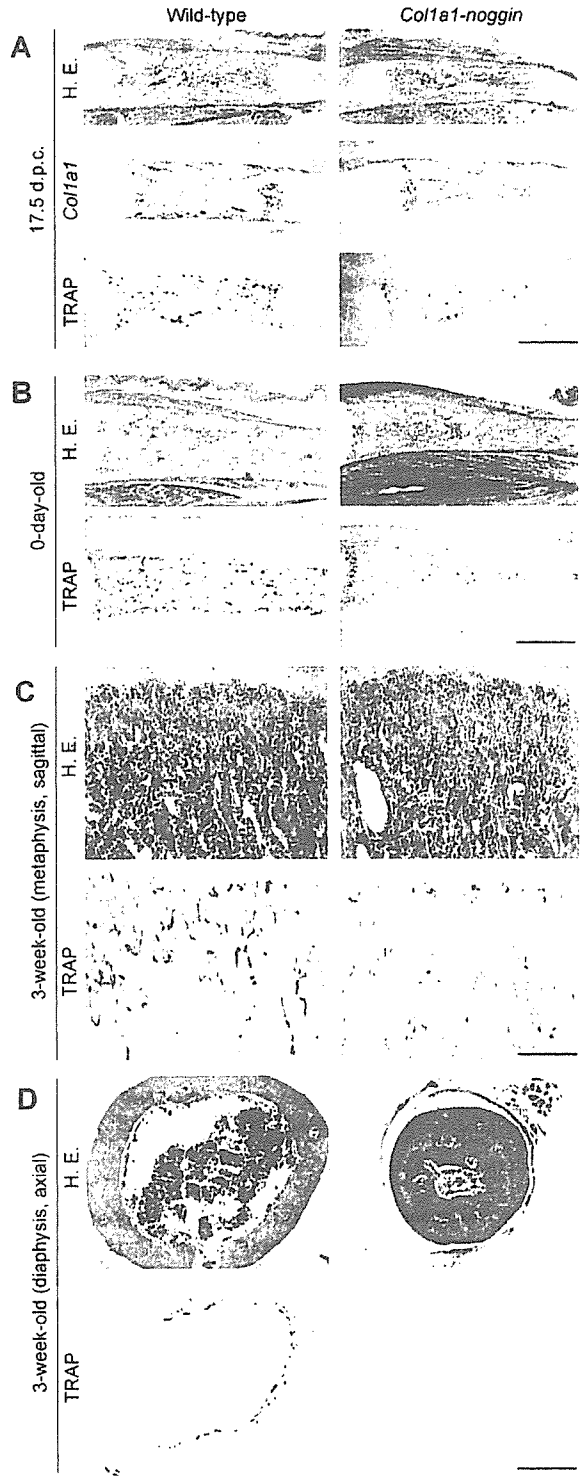

FIG. 4. Histological analysis of tibia of wildtype and *Col1a1-noggin* transgenic mice. (A) Semiserial sagittal sections prepared from 17.5 d.p.c. mice were stained with H&E, hybridized with *Col1a1* antisense cRNA probe (*Col1a1*), and stained for TRACP. Scale bar, 500 μm. (B) Sagittal sections from mice at birth. Semiserial sections were stained with H&E and for TRACP. Scale bar, 500 μm. (C) Sagittal sections of proximal metaphysis of tibias from 3-week-old mice. Semiserial sections were stained with H&E and for TRACP. Scale bar, 200 μm. (D) Axial sections of diaphysis of tibias from 3-week-old mice. Semiserial sections were stained with H&E and for TRACP. Scale bar, 200 μm.

nificant difference in the mineralization surface area per bone surface area (Fig. 5E). The data indicate that the bone formation rate was significantly decreased in the transgenic mice (Fig. 5F). These results suggest that overexpression of noggin in bone disturbs the function of osteoblasts.

The transgenic mice had a significantly lower osteoclast number per bone surface area and a significantly lower erosive surface area per bone surface area (Figs. 5G and 5H), suggesting that overexpression of noggin in bone inhibited osteoclastic bone resorption. The increased bone volume in *Col1a1-noggin* transgenic mice indicates that the decrease in bone resorption was greater than the decrease in bone formation.

Cortex of Col1a1-noggin transgenic mice was thick, but was woven and frequently suffered fractures

In the morphometric assays using the distal one third of the diaphysis of tibias of 3-week-old mice, total tissue volume was lower in *Col1a1-noggin* transgenic mice than in wildtype mice (Fig. 5I), but the cortical area in this region was significantly greater in transgenic mice (Figs. 5J and 5L). The marrow area was markedly lower in transgenic mice (Figs. 5K and 5L). Microscopic examination using polarized light revealed that the cortical bone of transgenic mice consisted mainly of immature bone (also known as woven bone, in which collagen fibers run in all directions), rather than the mature lamellar bone (which contains highly ordered parallel collagen fibers) found in the wildtype mice (Fig. 5L). Dynamic histomorphometric assays using consecutive labeling with tetracycline and calcein showed that bone formation rates were significantly decreased at the periosteal (Fig. 5M) and endosteal (Fig. 5N) surfaces of the diaphysis of tibias in 3-week-old *Col1a1-noggin* transgenic mice compared with wildtype mice. Together with the reduced osteoclast number at the endosteal surface of the noggin-transgenic tibial cortex (Fig. 4D), these results suggest that the presence of woven bone in the diaphyseal marrow spaces of noggin-transgenic mice was caused by failure to resorb initially formed immature bone and that the reduced cortical expansion in noggin-transgenic mice was caused by decreased periosteal modeling. Transgenic mice frequently suffered fractures at this region of the tibial shaft in the later stages of life, suggesting mechanical weakness of the bone (Fig. 5O). X-ray imaging of 8-week-old mice revealed that 7 of the 12 tibias of transgenic mice were broken, whereas none of the 12 tibias of wildtype mice were broken. This bone fragility in noggin-transgenic mice may be caused by a combination of impaired architecture and retention of immature woven bone.

Impaired osteoclast formation caused by noggin overexpression was rescued by BMP2 administration in vitro

To study the effects of noggin expressed by transgenic osteoblasts on osteoclast formation, we performed coculture experiments using primary osteoblasts prepared from calvariae of wildtype or *Col1a1-noggin* transgenic neonates and spleen cells from wildtype mice. The number of $TRACP^+$ osteoclasts (Figs. 6A and 6B) and the resorp-

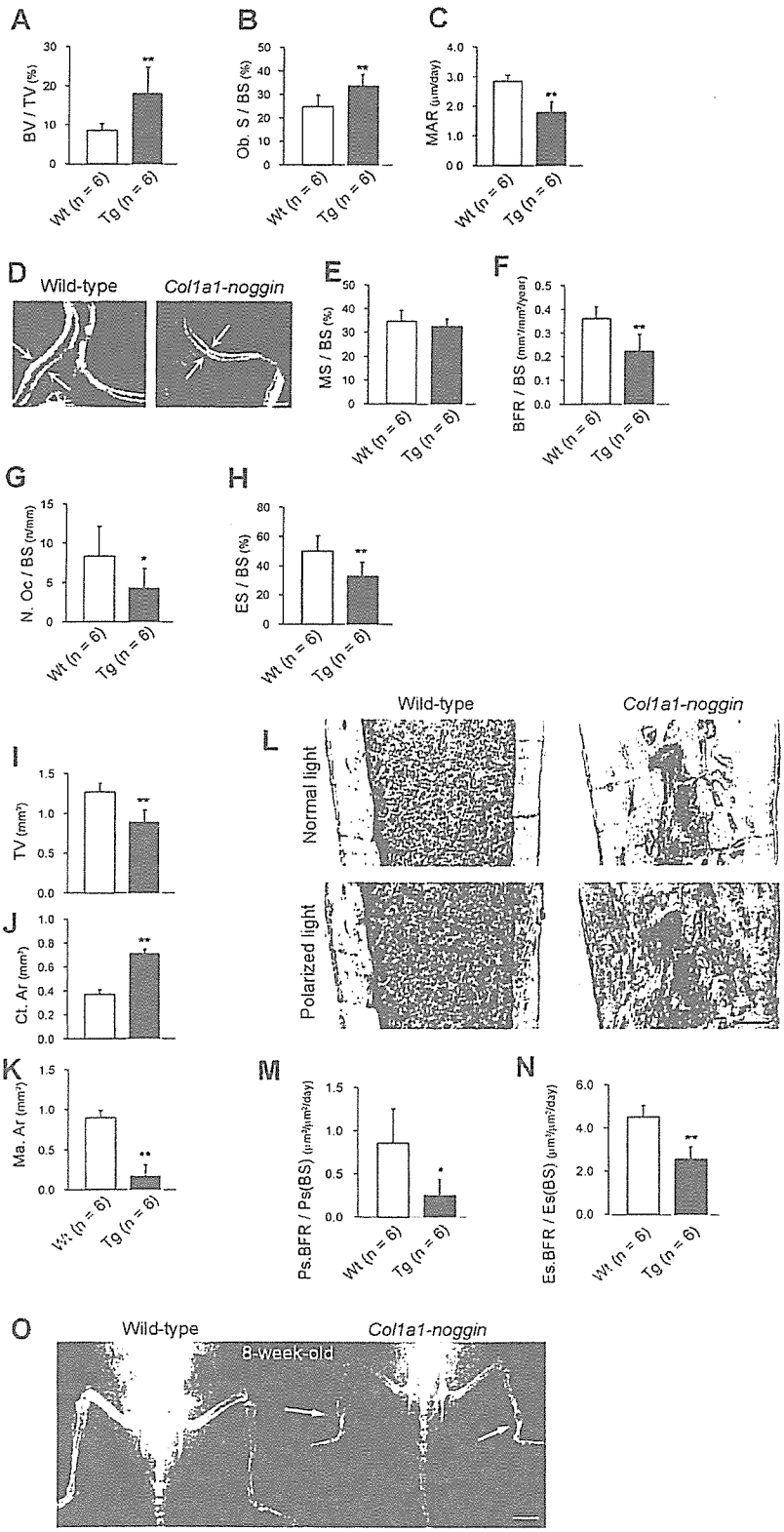

FIG. 5. Bone turnover and remodeling in wildtype and *Col1a1-noggin* transgenic mice. (A and B) Bone histomorphometric analysis of proximal metaphysis of tibia of 3-week-old mice. (A) Trabecular bone volume per tissue volume (BV/TV) and (B) osteoblast surface area per bone surface area (Ob.S/BS). (C–H) Bone histomorphometric analysis of fourth lumbar vertebral bodies of 3-week-old mice. (C) Mineral apposition rate (MAR). (D) Fluorescent micrograph of labeled mineralization fronts in the fourth lumbar vertebral bodies. *Arrows* indicate distance between the two consecutive labels. Scale bar, 20 μm. (E) Mineralizing surface area per bone surface area (MS/BS), and (F) bone formation rate per bone surface area (BFR/BS). (G) Osteoclast number per bone surface area (N.Oc/BS), and (H) eroded surface area per bone surface area (ES/BS). (I–N) Bone histomorphometric analysis of distal one third of diaphysis of tibias of 3-week-old mice. (I) TV, tissue volume; (J) Ct. Ar, cortical area; (K) Ma. Ar, marrow area. Sagittal histological sections of distal one third of diaphysis of tibias of 3-week-old mice were subjected to Villanueva bone staining. (L) Sections were viewed under a microscope using normal light and polarized light. Scale bar, 100 μm. (M) Periosteal bone formation rate per periosteal bone surface area [Ps. BFR/Ps(BS)]. (N) Endosteal bone formation rate per endosteal bone surface area [Es. BFR/Es(BS)]. (O) X-ray images of hind limbs of 8-week-old mice. Note fractures of tibias of *Col1a1-noggin* transgenic mice (white arrows). Scale bar, 5 mm. Error bars indicate means ± SD. $*p < 0.05$ and $**p < 0.01$ between wildtype and transgenic mice, as determined by *t*-test. Wt, wildtype mice; Tg, *Col1a1-noggin* transgenic mice.

tion of hydroxyapatite (Fig. 6C) were significantly lower for transgenic osteoblasts than for wildtype osteoblasts. In co-cultures with transgenic osteoblasts, numbers of $TRACP^+$ cells and osteoclastic resorption of hydroxyapatite were increased by addition of rhBMP2 to the medium in a dose-dependent manner. These results suggest that noggin inhibits osteoclastogenesis by attenuating BMP activity in *Col1a1-noggin* transgenic mice.

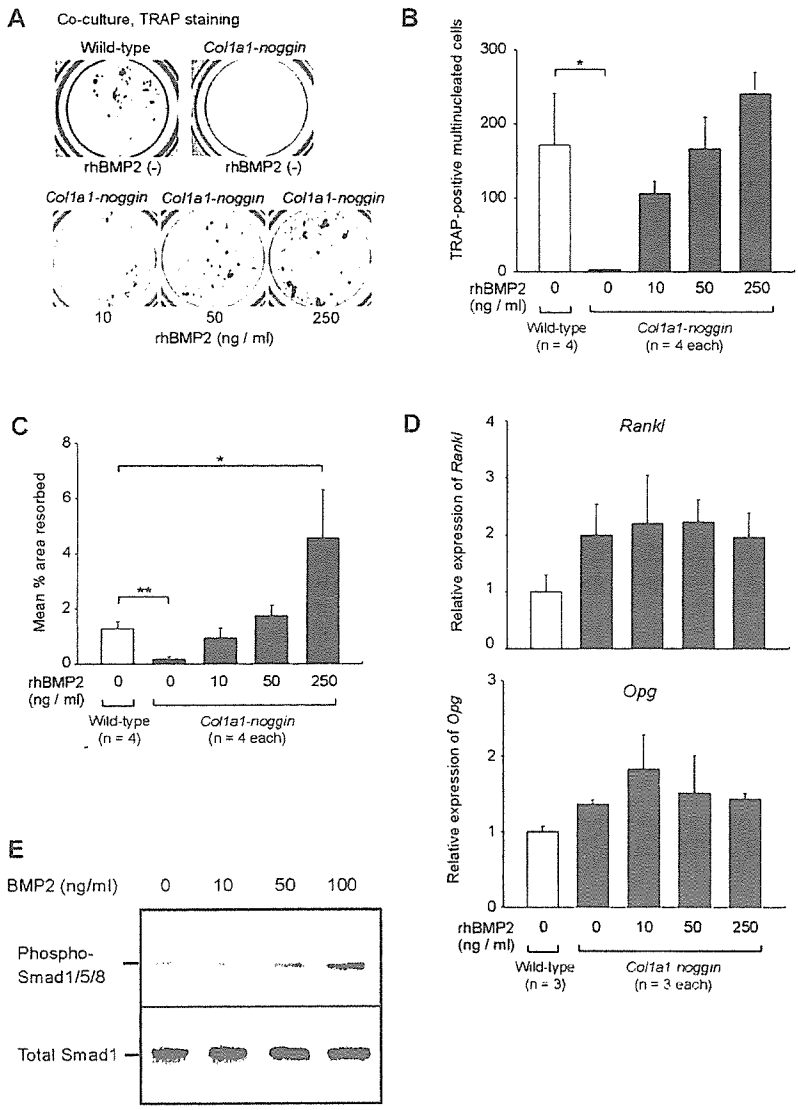

FIG. 6. Analysis of osteoclastogenesis in vitro using samples prepared from wildtype and *Col1a1-noggin* transgenic mice. (A) TRACP staining of osteoclasts in co-cultures of wildtype or *Col1a1-noggin* transgenic primary osteoblasts and wildtype spleen cells. Co-cultures containing transgenic osteoblasts were also performed in the presence of rhBMP2 at various concentrations. (B) Number of multinucleated TRACP$^+$ cells in co-cultures. Error bars indicate means ± SD. $*p < 0.05$, as determined by *t*-test. (C) Resorption of hydroxyapatite in co-cultures. Error bars indicate means ± SD. $*p < 0.05$ and $**p < 0.01$ between wildtype and transgenic mice, as determined by *t*-test. (D) Relative expression levels of *Rankl* and *Opg* mRNA in primary osteoblasts prepared from calvariae of neonate wildtype and *Col1a1-noggin* transgenic mice, measured by real-time RT-PCR. Expression levels of *Rankl* and *Opg* mRNA was also examined in *Col1a1-noggin* transgenic primary osteoblasts cultured in the presence of rhBMP2 at various concentrations for 3 days. The wildtype expression level was designated as 1. RT-PCR was performed three times. Data are presented as mean ± SD. (E) Activation of Smad pathways in bone marrow macrophages by BMP stimulation. Western blots of lysates from bone marrow macrophages incubated with rhBMP2 at various concentrations for 20 minutes. Blots were probed with antibodies against phospho-Smads 1/5/8 and Smad 1.

To examine whether the RANKL/OPG system was involved in changes in osteoclast numbers in *Col1a1-noggin* transgenic mice, we measured expression of *Rankl* and *Opg* mRNA in primary osteoblasts prepared from calvariae by performing real-time RT-PCR three times (Fig. 6D). Primary osteoblasts from *Col1a1-noggin* transgenic calvariae did not exhibit decreased expression of *Rankl* mRNA, and they exhibited only slightly increased expression of *Opg* mRNA. Treatment with rhBMP2 at various concentrations for 3 days did not much affect levels of *Rankl* or *Opg* mRNA in noggin-transgenic primary osteoblasts.

BMPs increased phosphorylation of Smads 1/5/8 in macrophage

We examined whether BMPs stimulate cells in the osteoclastic lineage by analyzing phosphorylation of R-Smads in those cells. Western blot analysis showed that bone marrow macrophages prepared by M-CSF treatment expressed Smad1 proteins. Amounts of phosphorylated Smads 1/5/8 in bone marrow macrophages were increased by 20-minute treatment with rhBMP2 in a dose-dependent manner (Fig. 6E), suggesting that BMPs directly activate Smad pathways in macrophages. In addition, immunohistochemistry using anti-phospho-Smads 1/5/8 (Fig. 2H) showed that in *Col1a1-Bmp4* transgenic mice, Smads 1/5/8 were phosphorylated in various types of cells including osteoclasts.

Cartilage-specific expression of BMP4 causes enlargement of bone and thickening of trabeculae during endochondral bone development

It has generally been believed that BMPs induce cartilage formation.[29] We previously reported that transgenic mice overexpressing growth and differentiation factor 5 (GDF5, also termed CDMP1, a member of BMP family) or BMP4 in chondrocytes exhibited expansion of cartilage.[22,30] To assess the effects of BMPs on bone formation when applied to cartilage during endochondral ossification, we examined bone of transgenic mice overexpressing BMP4 in chondrocytes under the control of the α2(XI) collagen promoter/

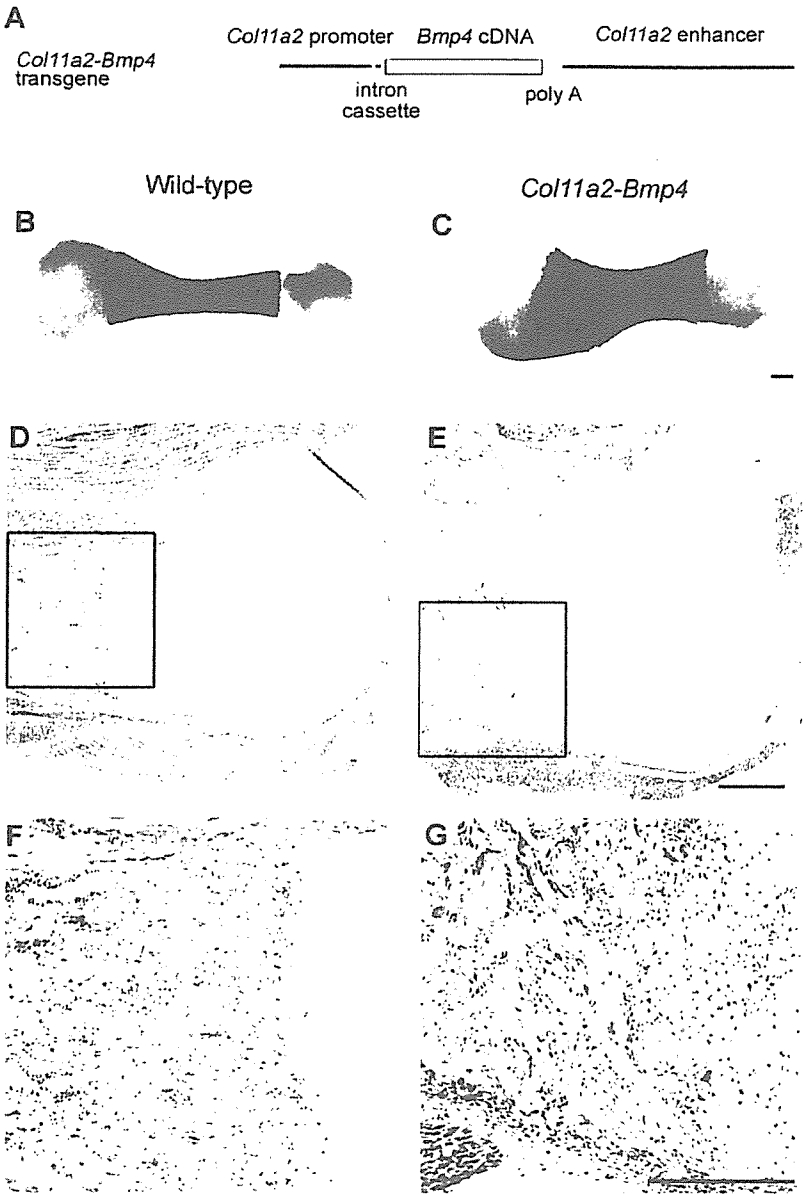

FIG. 7. Bone enlargement with thick trabeculae in *Coll1a2-Bmp4* transgenic mice. (A) Schematic representation of *Coll1a2-Bmp4* transgene construct. Humeri of (B) wildtype and (C) *Coll1a2-Bmp4* transgenic mice at 18.5 d.p.c. were stained with Alizarin red and Alcian blue. Scale bar, 200 μm. Histological analysis of proximal humerus of (D and F) wildtype and (E and G) *Coll1a2-Bmp4* transgenic mice at 18.5 d.p.c. H&E staining. Magnification of boxed regions in D and E are shown in F and G, respectively. Scale bar, 200 μm.

enhancer sequences (*Coll1a2-Bmp4* transgenic mice)[22] (Fig. 7A). At 18.5 d.p.c., epiphyseal cartilage of humeri in *Coll1a2-Bmp4* transgenic mice (Fig. 7C) had expanded compared with the wildtype (Fig. 7B). Ossification centers in the transgenic mice also expanded (Figs. 7B and 7C). Histological analysis further revealed that transgenic mice had thicker trabecular bone in marrow cavities than wildtype mice (Figs. 7D–7G). It seems that the large ossification centers with thick trabeculae in *Coll1a2-Bmp4* transgenic mice might be the result of an expanded cartilage template. These findings suggest that BMPs expressed in cartilage induce expansion of cartilage anlagen, resulting in expansion of bone.

DISCUSSION

In this study, we generated transgenic mice expressing BMP4 or noggin in osteoblasts under the control of the *Col1a1* promoter sequence. BMP overexpression in bone caused severe osteopenia, whereas noggin overexpression in bone resulted in thickening of trabecular and cortical bone. BMPs and noggin are secreted proteins and they diffuse in extracellular spaces. Thus, in *Col1a1-Bmp4* and *Col1a1-noggin* transgenic mice, in addition to autocrine action, BMP4 and noggin, respectively, produced by osteoblasts may also directly act on various cells in bone marrow cavities such as osteoclasts, stromal cells, and hematopoietic cells. In *Col1a1-noggin* transgenic mice, the bone formation rate was decreased, but the number of osteoblasts did not decrease, suggesting impairment of osteoblast function. Impairment of osteoblast function has previously been observed in mice in which BMP signaling in osteoblasts is blocked (e.g., mice with targeted disruption of BMP receptor type IA in osteoblasts)[11] and mice expressing dominant-negative BMP receptor type IB in osteoblasts.[10]

Those findings and these results suggest that, in *Col1a1-noggin* transgenic mice, noggin acts through an autocrine mechanism by preventing BMPs from interacting with BMP receptors on osteoblasts that overexpress noggin.

In addition to impairment of osteoblast function, *Col1a1-noggin* transgenic mice exhibited a significant decrease in osteoclast number. In a previous study, exogenous recombinant noggin attenuated osteoclast formation in stromal cell/hematopoietic cell co-cultures, and this effect is mediated by osteoblasts/stromal cells; this suggests that BMPs act on osteoclasts indirectly through osteoblasts or stromal cells.[31] In mice older than 10 months, conditional disruption of BMP receptor type IA in osteoblasts causes a decrease in the osteoclast number.[11] On the other hand, the osteoclast number was not decreased by expression of dominant-negative BMP receptor type IB in osteoblasts under the control of the 2.3-kb *Col1a1* promoter sequence that we used to direct noggin expression in this study.[10] In those mice, BMP signals may not be blocked in cells other than osteoblasts. Several in vitro studies suggest that BMPs also act on osteoclasts directly and that osteoclasts express BMP receptors.[13–15] Such findings suggest that, in *Col1a1-noggin* transgenic mice, noggin overexpressed by osteoblasts also acts on osteoclasts through paracrine action by preventing BMPs from interacting with BMP receptors on osteoclasts. This hypothesis is consistent with the present finding that *Rankl* expression in *Col1a1-noggin* transgenic primary osteoblasts was not decreased compared with wild-type and was not increased by incubation with rhBMP2 for 3 days or 6 h (data not shown), although it is possible that the *Rankl* expression level changed at other time-points during incubation with rhBMP2. This hypothesis is supported by the present finding that exogenous BMP2 increased phosphorylation of Smad1/5/8 in cultured bone marrow monocytes/macrophages. We speculate that BMPs also stimulate osteoclasts directly in vivo.

Impaired osteoclast formation in co-culture with *Col1a1-noggin* transgenic osteoblasts/spleen cells was rescued by adding rhBMP2, suggesting that noggin exerted their effects by attenuating BMP activity. Noggin binds with various degrees of affinity to BMPs 2, 4, 5, 6, and 7, growth differentiation factor 5 (GDF5), GDF6, and Vg1, but not to other members of the TGF-β family.[5,32,33] Noggin binds to BMP2 and BMP4 effectively and to BMP7 less tightly. Bone phenotype of *Col1a1-noggin* transgenic mice might be mainly caused by blocking activities of BMP2 and BMP4, although it is possible that blockage of activity of other BMPs contributed to abnormalities in *Col1a1-noggin* transgenic mice. These results do not exclude the possibility that some of the effects of noggin are independent of BMPs.

It has been reported that 4-week-old transgenic mice overexpressing noggin under the control of the 1.7-kb rat osteocalcin promoter exhibit decreased bone mass.[12] Transgenic mice overexpressing noggin under the control of the 1.3-kb murine osteocalcin promoter develop normally until they are 4 months old and exhibit decreased bone mass at 8 months of age.[34] The phenotypic difference between those mice and the present *Col1a1-noggin* transgenic mice may be caused by differences in transcriptional activity between osteocalcin and *Col1a1* promoters. The osteocalcin promoter directs noggin expression only in mineralizing osteoblasts, which represent a minor and localized fraction of all osteoblastic cells in situ.[34] The osteocalcin promoter directs strong expression at 4 and 8 weeks of age.[12] In contrast, the 2.3-kb *Col1a1* promoter sequence directs expression in most osteoblasts[23] beginning in the embryonic stage (Figs. 1A and 1B). This helps explain why bone abnormalities in the present *Col1a1-noggin* transgenic mice were detectable beginning in the embryonic stage at 17.5 d.p.c. It has been reported that, in osteoblasts, transcriptional activity of the *Col1a1* promoter is much stronger than that of the osteocalcin promoter.[21] From these lines of observation, we speculate that strong activities of the *Col1a1* promoter sequence might be important for disclosure of the effect of BMPs on osteoclasts, especially for direct effects through paracrine mechanism.

The reduced bone formation and resorption associated with frequent fractures in *Col1a1-noggin* transgenic mice suggests important functions of BMP signals in bone. Because noggin overexpression affected both osteoblast function and osteoclast number in this study, we speculate that a physiological function of BMPs in bone is acceleration of bone turnover, which improves the quality and mechanical strength of bone. Strict control of BMP activity may be necessary for formation of high-quality bone, as suggested by the present finding that both *Col1a1-noggin* and *Col1a1-Bmp4* transgenic mice exhibited fragile bone.

In this study, *Col11a2-Bmp4* transgenic mice exhibited expanded cartilage as well as expanded bone containing thick trabeculae. *Col11a2* promoter/enhancer sequences direct expression in mesenchymal condensation and cartilage, but not in bone.[24,25] These results are consistent with our previous report that noggin overexpression in cartilage under the control of the *Col11a2* promoter/enhancer sequences caused cartilage and bone to become very hypoplastic.[22] We have not analyzed the mechanism by which expansion of cartilage led to bone enlargement and thickening. In addition to its effects as anlagen, expanded cartilage may produce signaling molecules that promote enlargement of bone. The events observed in the skeleton of the present *Col11a2-Bmp4* transgenic mice may resemble the processes that occur during healing of fracture treated with BMPs. BMPs have been used to promote fracture healing.[18–20] BMPs applied to fracture sites may act on mesenchymal cells and chondrocytes, causing formation of a large cartilaginous callus that promotes solid bone formation. Exogenous BMP also contribute to bone formation by stimulating osteoblast function and remodeling. The bone phenotype of *Col1a1-Bmp4* transgenic mice suggest that persistent application of large amount of BMP4 to bone stimulate osteoclastic bone resorption continuously and cause bone loss. These finding may be helpful in planning schedule of BMP application to further improve clinical results of fracture treatment.

ACKNOWLEDGMENTS

The authors thank Akira Myoui for providing critical comments, Takao Iwai, Kaori Sudo, Mari Shinkawa, Yu-

suke Hashimoto, and Hideki Tsuboi for commitment to this study, Dr Benoit de Crombrugghe for providing the *Col1a1* promoter, and Akemi Ito for performing the histomorphometrical analysis. This study was supported in part by Scientific Research Grants 15390458 and 17659467 from the Ministry of Education, Science and Culture of Japan, by Health and Labor Sciences Research Grants of Japan, and by the Osaka Medical Research Foundation for Incurable Diseases.

REFERENCES

1. Urist MR 1965 Bone: Formation by autoinduction. Science **150**:893–899.
2. Wozney JM, Rosen V, Celeste AJ, Mitsock LM, Whitters MJ, Kriz RW, Hewick RM, Wang EA 1988 Novel regulators of bone formation: Molecular clones and activities. Science **242**:1528–1534.
3. Shi Y, Massague J 2003 Mechanisms of TGF-β signaling from cell membrane to the nucleus. Cell **113**:685–700.
4. Balemans W, Van Hul W 2002 Extracellular regulation of BMP signaling in vertebrates: A cocktail of modulators. Dev Biol **250**:231–250.
5. Zimmerman LB, De Jesus-Escobar JM, Harland RM 1996 The Spemann organizer signal noggin binds and inactivates bone morphogenetic protein 4. Cell **86**:599–606.
6. Groppe J, Greenwald J, Wiater E, Rodriguez-Leon J, Economides AN, Kwiatkowski W, Affolter M, Vale WW, Belmonte JC, Choe S 2002 Structural basis of BMP signalling inhibition by the cystine knot protein Noggin. Nature **420**:636–642.
7. Olsen BR, Reginato AM, Wang W 2000 Bone development. Annu Rev Cell Dev Biol **16**:191–220.
8. Suda T, Takahashi N, Udagawa N, Jimi E, Gillespie MT, Martin TJ 1999 Modulation of osteoclast differentiation and function by the new members of the tumor necrosis factor receptor and ligand families. Endocr Rev **20**:345–357.
9. Zhao GQ 2003 Consequences of knocking out BMP signaling in the mouse. Genesis **35**:43–56.
10. Zhao M, Harris SE, Horn D, Geng Z, Nishimura R, Mundy GR, Chen D 2002 Bone morphogenetic protein receptor signaling is necessary for normal murine postnatal bone formation. J Cell Biol **157**:1049–1060.
11. Mishina Y, Starbuck MW, Gentile MA, Fukuda T, Kasparcova V, Seedor JG, Hanks MC, Amling M, Pinero GJ, Harada S, Behringer RR 2004 Bone morphogenetic protein type IA receptor signaling regulates postnatal osteoblast function and bone remodeling. J Biol Chem **279**:27560–27566.
12. Devlin RD, Du Z, Pereira RC, Kimble RB, Economides AN, Jorgetti V, Canalis E 2003 Skeletal overexpression of noggin results in osteopenia and reduced bone formation. Endocrinology **144**:1972–1978.
13. Kaneko H, Arakawa T, Mano H, Kaneda T, Ogasawara A, Nakagawa M, Toyama Y, Yabe Y, Kumegawa M, Hakeda Y 2000 Direct stimulation of osteoclastic bone resorption by bone morphogenetic protein (BMP)-2 and expression of BMP receptors in mature osteoclasts. Bone **27**:479–486.
14. Itoh K, Udagawa N, Katagiri T, Iemura S, Ueno N, Yasuda H, Higashio K, Quinn JM, Gillespie MT, Martin TJ, Suda T, Takahashi N 2001 Bone morphogenetic protein 2 stimulates osteoclast differentiation and survival supported by receptor activator of nuclear factor-kappaB ligand. Endocrinology **142**:3656–3662.
15. Kanatani M, Sugimoto T, Kaji H, Kobayashi T, Nishiyama K, Fukase M, Kumegawa M, Chihara K 1995 Stimulatory effect of bone morphogenetic protein-2 on osteoclast-like cell formation and bone-resorbing activity. J Bone Miner Res **10**:1681–1690.
16. Reddi AH 1997 Bone morphogenetic proteins: An unconventional approach to isolation of first mammalian morphogens. Cytokine Growth Factor Rev **8**:11–20.
17. Vortkamp A, Pathi S, Peretti GM, Caruso EM, Zaleske DJ, Tabin CJ 1998 Recapitulation of signals regulating embryonic bone formation during postnatal growth and in fracture repair. Mech Dev **71**:65–76.
18. Govender S, Csimma C, Genant HK, Valentin-Opran A, Amit Y, Arbel R, Aro H, Atar D, Bishay M, Borner MG, Chiron P, Choong P, Cinats J, Courtenay B, Feibel R, Geulette B, Gravel C, Haas N, Raschke M, Hammacher E, van der Velde D, Hardy P, Holt M, Josten C, Ketterl RL, Lindeque B, Lob G, Mathevon H, McCoy G, Marsh D, Miller R, Munting E, Oevre S, Nordsletten L, Patel A, Pohl A, Rennie W, Reynders P, Rommens PM, Rondia J, Rossouw WC, Daneel PJ, Ruff S, Ruter A, Santavirta S, Schildhauer TA, Gekle C, Schnettler R, Segal D, Seiler H, Snowdowne RB, Stapert J, Taglang G, Verdonk R, Vogels L, Weckbach A, Wentzensen A, Wisniewski T 2002 Recombinant human bone morphogenetic protein-2 for treatment of open tibial fractures: A prospective, controlled, randomized study of four hundred and fifty patients. J Bone Joint Surg Am **84**:2123–2134.
19. Friedlaender GE, Perry CR, Cole JD, Cook SD, Cierny G, Muschler GF, Zych GA, Calhoun JH, LaForte AJ, Yin S 2001 Osteogenic protein-1 (bone morphogenetic protein-7) in the treatment of tibial nonunions. J Bone Joint Surg Am **83**(Suppl 1):S151–S158.
20. Einhorn TA 2003 Clinical applications of recombinant human BMPs: Early experience and future development. J Bone Joint Surg Am **85**(Suppl 3):82–88.
21. Dacquin R, Starbuck M, Schinke T, Karsenty G 2002 Mouse α1(I)-collagen promoter is the best known promoter to drive efficient Cre recombinase expression in osteoblast. Dev Dyn **224**:245–251.
22. Tsumaki N, Nakase T, Miyaji T, Kakiuchi M, Kimura T, Ochi T, Yoshikawa H 2002 Bone morphogenetic protein signals are required for cartilage formation and differently regulate joint development during skeletogenesis. J Bone Miner Res **17**:898–906.
23. Rossert J, Eberspaecher H, de Crombrugghe B 1995 Separate *cis*-acting DNA elements of the mouse pro-α1(I) collagen promoter direct expression of reporter genes to different type I collagen-producing cells in transgenic mice. J Cell Biol **129**:1421–1432.
24. Tsumaki N, Kimura T, Matsui Y, Nakata K, Ochi T 1996 Separable *cis*-regulatory elements that contribute to tissue- and site-specific α2(XI) collagen gene expression in the embryonic mouse cartilage. J Cell Biol **134**:1573–1582.
25. Horiki M, Imamura T, Okamoto M, Hayashi M, Murai J, Myoui A, Ochi T, Miyazono K, Yoshikawa H, Tsumaki N 2004 Smad6/Smurf1 overexpression in cartilage delays chondrocyte hypertrophy and causes dwarfism with osteopenia. J Cell Biol **165**:433–445.
26. Kenner L, Hoebertz A, Beil T, Keon N, Karreth F, Eferl R, Scheuch H, Szremska A, Amling M, Schorpp-Kistner M, Angel P, Wagner EF 2004 Mice lacking JunB are osteopenic due to cell-autonomous osteoblast and osteoclast defects. J Cell Biol **164**:613–623.
27. Takahashi N, Udagawa N, Akatsu T, Tanaka H, Isogai Y, Suda T 1991 Deficiency of osteoclasts in osteopetrotic mice is due to a defect in the local microenvironment provided by osteoblastic cells. Endocrinology **128**:1792–1796.
28. Suda T, Jimi E, Nakamura I, Takahashi N 1997 Role of 1α,25-dihydroxyvitamin D3 in osteoclast differentiation and function. Methods Enzymol **282**:223–235.
29. Brunet LJ, McMahon JA, McMahon AP, Harland RM 1998 Noggin, cartilage morphogenesis, and joint formation in the mammalian skeleton. Science **280**:1455–1457.
30. Tsumaki N, Tanaka K, Arikawa-Hirasawa E, Nakase T, Kimura T, Thomas JT, Ochi T, Luyten FP, Yamada Y 1999 Role of CDMP-1 in skeletal morphogenesis: Promotion of mesenchymal cell recruitment and chondrocyte differentiation. J Cell Biol **144**:161–173.
31. Abe E, Yamamoto M, Taguchi Y, Lecka-Czernik B, O'Brien CA, Economides AN, Stahl N, Jilka RL, Manolagas SC 2000 Essential requirement of BMPs-2/4 for both osteoblast and